

## **Supplemental Data**

### **Proteomic and Genetic Approaches**

#### **Identify Syk as an AML Target**

**Cynthia K. Hahn, Jacob E. Berchuck, Kenneth N. Ross, Rose M. Kakoza, Karl Clauser, Anna C. Schinzel, Linda Ross, Ilene Galinsky, Tina N. Davis, Serena J. Silver, David E. Root, Richard M. Stone, Daniel J. DeAngelo, Martin Carroll, William C. Hahn, Steven A. Carr, Todd R. Golub, Andrew L. Kung, and Kimberly Stegmaier**

### **Supplemental Experimental Procedures**

#### **Cell Culture**

Primary patient AML blasts were collected from peripheral blood or bone marrow aspirate after obtaining patient informed consent under Dana-Farber Cancer Institute and the University of Pennsylvania Internal Review Board-approved protocols. Mononuclear cells were isolated using Ficoll-Paque Plus (Amersham Biosciences) and red blood cells lysed. Cryopreserved human bone marrow CD34+ cells were obtained from Poietics, and use of these materials is considered exempt as Human Subjects by the Dana-Farber Cancer Institute Internal Review Board.

HL-60, U937, Kasumi-1, and KG-1 were purchased from the American Type Culture Collection. THP-1, MOLM-14, 697, NALM-6, REH, RS4-11, SEMK2, and SUP-B15 were kindly provided by Dr. Scott Armstrong. DND-41, HPBALL, KOPTK1, MOLT-4, and PF-382 were all kindly provided by Dr. Jon Aster. All cell lines and primary patient cells were maintained in RPMI 1640 (Cellgro) supplemented with 1% penicillin-streptomycin and 10% fetal bovine serum (Sigma-Aldrich) at 37 °C with 5% CO<sub>2</sub>.

## Chemicals

Gefitinib (WuXi PharmaTech, Shanghai, China) and All-trans retinoic acid (ATRA) (Sigma-Aldrich) were dissolved in dimethyl sulfoxide (DMSO) at a concentration of 50 mM and 33.3 mM, respectively, and stored at -20 °C. R406 (Rigel Pharmaceuticals, Inc., San Francisco, CA) was resuspended in DMSO at a concentration of 10 mM and stored at -80 °C. After thawing, the R406 stock solution was kept in a desiccator at room temperature for up to one week. R788 was also kindly provided by Rigel Pharmaceuticals.

## Phosphoproteomic Studies

HL-60 cells ( $1 \times 10^9$ ) were treated in duplicate with 10  $\mu$ M gefitinib for 10 minutes.

The basics of the procedure were developed and described by Rush et al. (**Rush et al., 2005**). In our current protocol cells were lysed in 8 M urea / 20 mM Hepes containing phosphatase inhibitors. Upon reduction of the disulfide bonds and alkylation of cysteines with iodoacetamide, the lysate was split into two aliquots and diluted with 20 mM Hepes to 2 M or 0.5 M urea before digestion with trypsin or chymotrypsin, respectively. The total peptide mixtures were then desalted by Sep-Pak cartridge and resuspended in immunoprecipitation (IP) buffer, 50 mM MOPS/NaOH pH 7.2, 10 mM  $\text{Na}_2\text{PO}_4$ , 50 mM NaCl, along with four exogenous pTyr-containing peptides added as controls. IP was performed with a cocktail of three protein G agarose bead-bound phospho-tyrosine antibodies pY100 (Cell Signaling), 4G10 (UpState), and pY99 (Santa Cruz Biotechnology) to enrich for phosphotyrosine-containing peptides. Peptides captured by phospho-tyrosine antibodies were eluted under basic followed by acidic conditions. The IP eluates were analyzed by data-dependent LC-MS/MS using a

ThermoFisher LTQ-Orbitrap instrument. The Orbitrap MS scans provide 60K resolution and +/- 10ppm mass accuracy on precursor ions to achieve unambiguous peptide identification. Each peptide's site(s) of phosphorylation were uniquely mapped using the sequence information present in its ion trap MS/MS spectrum, unless it had several tyrosine residues and fragmented poorly. All MS and MS/MS data was processed using the Spectrum Mill software package (developed internally and commercialized by Agilent Technologies) which assigns peptide identity with < 1% false discovery rate using a target-decoy database search approach, maps phosphorylation sites, and quantitates using extracted ion chromatograms of each peptide precursor ion. Searches were performed using a sequence database consisting of the human subset of NCBI nr supplemented with common contaminating proteins (porcine trypsin, bovine serum albumin, sheep keratin) with a precursor MH<sup>+</sup> tolerance of +/-0.5 Da, a fragment MH<sup>+</sup> tolerance of +/-0.7 Da, fixed modification of cysteine by iodoacetamide, and certain variable modifications allowed (phosphorylation of tyrosine, serine and threonine, oxidation of methionine, deamidation of asparagine, pyroglutamic acid formation at peptide N-terminal glutamines, and carbamylation of peptide N-termini by urea). The peak area in the extracted ion chromatogram (XIC) of each precursor ion was calculated automatically by the Spectrum Mill software with narrow windows around each individual member of the isotope cluster. Peak widths in both the time and m/z domains are dynamically determined based on MS scan resolution, precursor charge and m/z subject to quality metrics on the relative distribution of the peaks in the isotope cluster vs. theoretical.

## RNA-interference Screening

HL-60 were arrayed in 384-well tissue culture plates in 30  $\mu$ l of medium at 15,000 cells/well using a BioTek MicroFill Microplate Dispenser and incubated overnight at 37  $^{\circ}$ C with 5% CO<sub>2</sub>. Polybrene (Sigma) was added using a BioTek MicroFill Microplate Dispenser to a final concentration of 8  $\mu$ g/ml. High-throughput screening was performed in quadruplicate at the RNAi Platform in the Broad Institute of Harvard and MIT using a kinase-directed lentiviral sub-library of the RNAi Consortium shRNA library (<http://www.broad.mit.edu/rnai/trc/lib>) which contains 3-5 hairpins per human kinase as previously described (**Moffat et al., 2006**). A Perkin Elmer Evolution P3 Precision Dispenser added 2.5  $\mu$ l virus to 360 wells on each plate, reserving 24 uninfected wells for chemical controls. Plates were spun for 30 minutes at 2250 rpm and incubated at 37  $^{\circ}$ C with 5% CO<sub>2</sub> for 48 hours. Selection was performed with a Zymark Rapid Plate 96 on three replicates with 1  $\mu$ g/ml puromycin (Sigma) and medium was changed on the other replicate to serve as an unselected control. At this time point, the following controls were added to the uninfected wells on each 384-well screen plate: cells only (8 wells), 1  $\mu$ M ATRA (8 wells), and 25  $\mu$ M gefitinib (8 wells). The plates were incubated for 72 hours at 37  $^{\circ}$ C with 5% CO<sub>2</sub>. A Promega Cell-Titer Glo ATP-based assay was performed on a puromycin selected and an unselected replicate using 10  $\mu$ l Cell-Titer Glo reagent per well. GE-HTS was carried out on two replicates as previously described (**Peck et al., 2006; Stegmaier et al., 2004**) and as detailed below. We used a 19-gene signature (**Table S2**) containing genes that distinguish AML from either neutrophil or monocyte with  $p < 0.05$  by t-test and distinguish undifferentiated versus differentiated HL-60 with either ATRA, PMA, or VitD with  $p < 0.05$  by t-test.

A secondary screen was performed as described above in the primary RNAi screen methods with the following exceptions: HL-60 and U937 cells were plated at 15,000 cells/well and 4,500 cells/well, respectively. Two lentiviral library plates containing shRNAs that scored in the primary screen as well as newly available shRNAs created by the TRC against hits were screened in five replicates. An expanded 32-gene signature (**Table S3**) was also used in the secondary screen.

### *Gene Expression-based High-throughput Screening (GE-HTS)*

#### *RNA Extraction and Reverse Transcription*

Cells were lysed with 25  $\mu$ l of lysis buffer for 20 minutes at room temperature, lysate transferred to a 384-well oligo-dT coated plate, and lysate incubated for one hour at room temperature. Reverse transcription was performed in a 5  $\mu$ l MMLV reaction (Promega) for 1.5 hours at 37 °C. Lysis buffers and 384-well oligo-dT plates were purchased from Qiagen.

#### *Ligation Mediated Amplification (LMA)*

After the reverse transcription reaction, solutions were removed by centrifugation into an absorbent towel. Signature gene-specific oligonucleotide probes were hybridized to the cDNA using 2 nM of each probe and Taq ligase buffer (New England Biolabs) in a 5  $\mu$ l reaction. Upstream probes contained the T7 primer site, Luminex designed FlexMap barcode tag (24nt), and gene-specific sequence (20nt). Downstream probes were phosphorylated at the 5' end and contained gene specific sequence (20nt) followed by the T3 primer site. Gene specific sequence was chosen such that the 20 base pair sequences of the two probes contain similar base composition, minimal repeats, and C-G, G-C, C-C, or G-G juxtaposing nucleotides. Hybridization was performed at 95 °C for

two minutes followed by 50 °C for one hour. Excess probe was then removed. Probes were ligated in a 5 µl reaction using Taq DNA ligase (New England Biolabs) at 45 °C for one hour followed by incubation at 65 °C for 10 minutes. Excess ligation mix was removed. The ligated products were amplified with the universal T3 primer (5'-ATT AAC CCT CAC TAA AGG GA-3') and universal biotinylated T7 primer (5'-TAA TAC GAC TCA CTA TAG GG-3') (Integrated DNA Technologies) using HotStarTaq DNA Polymerase (Qiagen) in a 5 µl reaction. PCR was performed at 92 °C for 9 minutes, followed by 34 cycles of denaturation at 92 °C for 30 seconds, annealing at 55 °C for 30 seconds, and extension at 72 °C for 30 seconds.

#### *Amplicon Detection*

xMAP Multi-Analyte COOH microspheres (Luminex, Austin, Texas, United States) (2.5 million) were coupled to complementary FlexMap barcode sequence (4 µM) with 2.5 µl of 10 mg/ml 1-ethyl-3-(3-dimethylaminopropyl)-carbodiimide hydrochloride (EDC) (Pierce) in 25 µl 0.1 M 2-(N-morpholino) ethanesulfonic acid, pH 4.5 (MES) buffer (Sigma) for 30 minutes and then the coupling reaction repeated. Microspheres were washed sequentially with 0.02% Tween-20, 0.1% SDS, and TE (pH 8) and resuspended in 50 µl of TE (pH 8). Next, LMA products were hybridized to microspheres by incubating 2,500 of each microsphere in 18 µl of 1.5X TMAC [(4.5 M tetramethylammonium chloride, 0.15% N-lauryl sarcosine, 75 mM Tris-HCl (pH 8), and 6 mM EDTA (pH 8))] and 5 µl of TE (pH 8) at 95 °C for two minutes and then 45 °C for one hour. For detection, the sample was incubated with 10 µl of streptavidin-phycoerythrin (SA-PE) (Invitrogen) (1% SA-PE in 1X TMAC [(3 M tetramethylammonium chloride, 0.1% N-lauryl sarcosine, 50 mM Tris-HCl (pH 8), and 4 mM EDTA (pH 8))] for five minutes at 45 °C and then washed twice and resuspended

with 1X TMAC. Dual-color fluorescence was detected with a Luminex high-throughput detection instrument. A minimum of 100 events was recorded for each microsphere and median fluorescent intensities (MFI) computed.

### *Data Analysis and Hairpin Hit Selection*

The median fluorescence level for each gene (where each gene was represented by a particular bead color) from the Luminex detector was used as a measure of the gene's expression. To maximize consistency between and within plates, we normalized genes by using the expression ratio between each gene and the reference gene *GAPDH*. Wells with technical failures or dead cells were filtered from further analysis by using *GAPDH* expression levels as a proxy for cell viability. Filtering is important because ratios with the reference gene *GAPDH* were used for subsequent analysis and we needed to eliminate wells where reference gene expression was nominally zero (379 wells). Plate specific reference filtering levels were set to be equal to the median of each plate's untreated HL-60 negative control wells minus four times their median absolute deviation (MAD). This screen also had viability data available for filtering and filtered out shRNA wells where the +Puromycin / -Puromycin ratio was less than 0.75 (1294 wells). There were also some shRNA wells that were flagged by the RNAi Platform as "failure to clone" that were removed from consideration (750 wells). For this screen, a total of 1693 out of 11520 shRNA wells were filtered by one or more of reference gene levels, viability ratios, or library flags. After filtering, each measurement was scaled using the robust Z-Score to further reduce plate-to-plate variation of measurements within the screen. The robust Z-Score normalizes the raw ratios for each gene in each well by assuming that the majority of shRNAs are inactive and can supplement any negative controls.

$$Z_i = \frac{x_i - m_p}{MAD_p}$$

where  $m_p$  is the median of the shRNA wells and negative controls (HL-60 wells) for plate  $p$  and  $MAD_p$  is the median absolute deviation of the shRNA and negative controls from the median. The robust Z-Score has the advantage over the traditional Z-Score in that it is relatively insensitive to statistical outliers.

After normalization, we used a combination of the Summed Score, Weighted Summed Score, Naïve Bayes, K-Nearest Neighbor (KNN), and Support Vector Machine (SVM) metrics to identify candidate AML differentiation-associated genes. An shRNA was considered a hit if the hairpin was classified as being more like gefitinib-treated controls than untreated HL-60 controls by all five methods. shRNAs are classified as “gefitinib-like” when the composite probability for Naïve Bayes, Summed Score or Weighted Summed Score methods has  $p=0.98$  that they are “gefitinib-like” or both replicates in KNN or SVM were classified as “gefitinib-like”. Approximately 2% of the hairpins that passed filtering fit this criterion for being called a hit. Genes that were flagged by multiple hairpins were also given priority for follow-up in the secondary screen.

The Summed Score metric combined expression ratios by summing them with a sign determined by the expected direction of regulation of the gefitinib-treated positive controls. The Weighted Summed Score metric is a variant of the Summed Score metric that combines expression ratios by summing them with a weight and sign determined by the signal-to-noise ratio of the gefitinib-treated positive controls and the untreated HL-60 negative controls. Signal-to-noise ratio is defined by:

$$W_i = \frac{\mu_{i1} - \mu_{i2}}{\sigma_{i1} + \sigma_{i2}}$$



where  $\mu_{i1}$  represents the mean expression of samples from class 1 for feature  $i$  and  $\sigma_{i1}$  represents the standard deviation of class 1 for feature  $i$  (**Golub et al., 1999**). Composite scores for both the Summed Score and Weighted Summed Score were formed by finding the average of the scores from the two replicates. Each shRNA's Summed Score and Weighted Summed Score was assigned a probability that the shRNA caused the cells to have an expression signature like those for the gefitinib-treated control wells. The calculation of the probability was based upon finding the Bayesian probability density of the score using normal distributions to model each of two classes of controls:

$$p(C = c | X = x) = \frac{p(C = c)p(X = x | C = c)}{p(X = x)}, \text{ where}$$

$$p(X = x | C = c) = N(x; \mu_c, \sigma_c)$$

$N(x; \mu_c, \sigma_c)$  was the probability density function for a normal (or Gaussian) distribution with mean  $\mu_c$  and standard deviation  $\sigma_c$  (**Duda and Hart, 1973**). The parameters for the Gaussian distribution were trained on the positive and negative controls and  $p(C=c)$  was the *a priori* probability of class  $c$  controls (in this case, we assumed the positive and negative controls have equal *a priori* probabilities). Composite probabilities were found by taking the product of the probabilities for the two replicates (but leaving out filtered replicates) and renormalizing the probabilities to ensure that the probability that the perturbation is a positive control and the probability that the perturbation is a negative control sum to one. Hairpins were ranked for follow-up according to the probability that they looked like the gefitinib-treated positive control.

A Naïve Bayes classifier was also used to evaluate the expression signatures for the hairpins. The Naïve Bayes classifier is based upon the Bayes probability rule and

naïvely assumes that the features are independent within each class. The independence assumption greatly simplifies the calculation of the class probabilities and has been shown to work well even in cases where the features have significant dependencies. The probabilities are calculated as follows:

$$p(C = c | \mathbf{X} = \mathbf{x}) = \frac{p(C = c)p(\mathbf{X} = \mathbf{x} | C = c)}{p(\mathbf{X} = \mathbf{x})}, \text{ where}$$
$$p(\mathbf{X} = \mathbf{x} | C = c) = \prod_i p(X_i = x_i | C = c)$$

for continuous values like the gene expression ratios  $p(X_i=x_i|C=c)$  a kernel distribution was formed out of a mixture of Gaussians (**John and P., 1995**). The parameters for the distribution for each class  $c$  and each feature  $i$  are trained using the controls for the screen. The overall probability for each shRNA is found by multiplying the probabilities for the individual replicates (leaving out filtered replicates) and renormalizing the probabilities so the two classes sum to one. shRNAs were ranked for follow-up according to the probability that they looked like a gefitinib-treated positive control.

The K-Nearest-Neighbor (KNN) classifier assigns samples to the class most frequently represented among the  $k$  nearest control samples (**Duda and Hart, 1973**). A KNN predictor was trained using the vehicle- and gefitinib-treated control samples and the shRNA-treated wells were tested using  $k=3$  with a Pearson correlation for the distance metric and weights for the neighbors based upon the Pearson distance. A modified version of KNN method was used here where the genes were given weights based upon their signal-to-noise ratio in the control samples.

A Support Vector Machine (SVM) classifier is a computationally efficient way of identifying separating hyperplanes in a high dimensional feature space. SVM maps

input vectors to a higher dimensional space where a maximal separating hyperplane is constructed. Parallel hyperplanes are constructed on each side of the hyperplane that separates the data. The selected separating hyperplane is the hyperplane that maximizes the distance between the parallel hyperplanes. The SVM assumes that a larger margin or distance between the parallel hyperplanes results in a classifier with a better generalization error (**Vapnik, 1998**). The SVM used a radial basis function kernel with parameters trained using the positive and negative controls in a cross-validation loop to test parameters in a grid-based search. Once the SVM parameters were selected all the positive and negative controls were used to train an SVM that was used to test the shRNA wells.

### **Lentiviral Vectors and Infection**

Oligonucleotides encoding shRNAs were cloned into pLKO.1 as described previously (**Moffat et al., 2006**). Sequences targeted by each SYK shRNA are listed in **Table S6**. For large scale infections, 500,000 293T cells were plated in 6 cm plates and transfected 24 hours later with 1 µg DNA from lentiviral backbone vector and packaging plasmids (pCMVdeltaR8.91 and pMD.G) according to FuGENE 6 (Roche) protocol. Medium was changed to RPMI 1640 24 hours post-transfection and viral supernatant was harvested and filtered 48 hours post-transfection. Typical lentiviral titers were  $1 \times 10^7$  IU/ml. Seven million HL-60 cells, 3.5 million MOLM-14 or U937 cells, and 5 million KG-1 cells were infected for two hours at 37 °C with 2 ml lentivirus and 8 µg/ml polybrene (Sigma). The volume was increased to 10 ml using RPMI 1640 and cells were selected 48 hours later with 1 µg/ml puromycin (Sigma).

To generate the TEL-Syk construct, RT-PCR was used to isolate the sequences encoding amino acids 1-336 of human ETV6 (TEL) and amino acids 266-635 of human Syk. The assembled cDNA was subcloned in place of mCherry in the lentiviral plasmid FUW-Luc-mCherry-puro (**Kimbrel et al., 2009**) to give the plasmid FUW-Luc-TEL-SYK-puro. VSVG-pseudotyped virus was produced by co-transfection of 293T cells along with the helper plasmids delta8.9 and CMV-VSVG. Infection of MOLM-14 was performed as above.

## **Differentiation Studies**

### *Morphological Evaluation*

Changes in cellular morphology were evaluated by May-Grunwald Giemsa staining (Sigma) after treatment with compounds or shRNA under light microscopy with oil with an Olympus BX41 microscope and Q-capture software at 1000X magnification.

### *Nitro-blue Tetrazolium (NBT) Reduction Assay*

NBT reduction assays were performed in triplicate. Compound-treated cells were compared to DMSO-treated controls after three days of treatment. Cells were incubated at 37 °C for 1 hour in a mixture containing total medium, 0.1% NBT (Sigma), and 1 µg/ml TPA (12-O-tetradecanoylphorbol-13-acetate; Sigma). The percentage of blue cells was counted by light microscopy for at least 200 cells per sample. Drug-treated cells were compared with DMSO-treated cells with a one-tailed t-test analysis assuming two samples with unequal variance.

### *Flow Cytometry*

For analysis of mature myeloid cell-surface markers, cells were stained with 1:25 CD11b-FITC (Beckman Coulter IM0530U) and 1:25 CD14-PE (Beckman Coulter IOTest IM0650U) for 30 minutes. Cells were detected by flow cytometry (Beckman Cytomics FC500) and data analyzed using the FlowJo software package (Tree Star). Fluorescence gating was set based on single-stained mouse Ig  $\kappa$  compensation bead fluorescence intensity (BD Biosciences #552843).

### *Gene Expression Studies*

Marker genes for myeloid differentiation were chosen using previously published Affymetrix data sets containing primary AML cells, normal human neutrophils, normal human monocytes, and the HL-60 AML cell line differentiated with either ATRA, phorbol 12-myristate 13-acetate (PMA), or 1,25-dihydroxyvitamin D3 (vitD) (**Stegmaier et al., 2004**). We selected an initial collection of 19 genes used in the RNAi primary screen and then an expanded group of 32 genes (**Tables S2 and S3**). These genes distinguish AML from either neutrophil or monocyte with  $p < 0.05$  by t-test and distinguish undifferentiated versus differentiated HL-60 with either ATRA, PMA, or VitD with  $p < 0.05$  by t-test. The GE-HTS assay was performed as detailed above. Briefly, mRNAs are captured on 384-well plates coated in oligo-dT and reverse transcribed to create cDNA. Then, ligation-mediated amplification (LMA) is performed to amplify marker genes, and amplicons are detected by fluorescent bead-based flow cytometry.

### **Viability Assay**

Viability experiments were performed in 384-well format in a minimum of four replicates using the Promega Cell-Titer Glo ATP-based assay per the manufacturer's instructions.

Leukemia cell lines were evaluated at 3 and 6 days with R406 in a two-fold dilution to establish the drug concentrations that reduced cell viability to 50 percent of the vehicle controls ( $IC_{50}$ ). Values for  $IC_{50}$  were calculated by interpolating a natural cubic spline fit to the measured viability data in R (using the spline function). The natural spline requires that the second derivative of the interpolated curve equal zero at the endpoints of the interval of interpolation. The  $IC_{50}$  value was found by evaluating in R the interpolated spline at 0.5 using the approx function.

### **Apoptosis Studies**

MOLM-14 and KG-1 cells were treated in triplicate with DMSO versus R406 for 6 days. Annexin V FITC/PI staining was performed with the Annexin V: FITC Apoptosis Detection Kit I (BD Pharmingen). Cells were analyzed by flow cytometry with a FACScan flow cytometer (Becton Dickinson) and CELLQuest analytical software.

### **Methylcellulose Colony Forming Assay**

For the RNAi studies, KG-1 and MOLM-14 cells were infected with shRNA directed against a luciferase control or *SYK* (three unique constructs) and selected 48 hours later with puromycin. After 48 hours of selection, cells were recounted by trypan blue exclusion and a total of  $3 \times 10^4$  cells were plated at 1:10 (vol/vol) in methylcellulose (ClonaCell-TCS Medium, 03814) with 1% penicillin-streptomycin and appropriate drug treatment. 1.1ml of methylcellulose was added to each 35 mm plate. Plates were incubated at 37 °C and 5% CO<sub>2</sub> in a humidified incubator and colony numbers counted for each plate 8 days later.

For pharmacological treatment of primary AML, AML cell lines, and normal CD34+ myeloid progenitor studies, cells were treated with R406 or matched vehicle control for 48 hours in liquid culture. After 48 hours, an equal number of cells (ranging from 2 - 7.5 x 10<sup>3</sup> depending on the cell sample) were plated at 1:10 (vol/vol) in MethoCult GF+H4435 methylcellulose (StemCell Technologies, #04445) with 1% penicillin-streptomycin and appropriate drug treatment. Plates were incubated at 37 °C and 5% CO<sub>2</sub> in a humidified incubator and colony numbers counted for each plate 8-17 days later.

### **Real-time RT-PCR**

Total RNA was isolated using TRIZOL reagent (Invitrogen) and cDNA was synthesized from 1 µg of total RNA using SuperScript III Reverse Transcriptase (Invitrogen) and oligo d(T)<sub>16</sub> primers in a 20 µl reaction system. One µl of 1:5 diluted cDNA was analyzed in the real-time quantitative PCR reactions prepared with TaqMan Universal Master Mix (Applied Biosystems). Each sample was assessed in triplicate to ensure reproducibility of the quantitative measurements. RPL13A expression was evaluated for each sample as a control for total RNA. Primers and probes for real-time RT-PCR were obtained from Applied Biosystems (RPL13A # Hs01926559\_g1, and SYK Hs00895374\_m1).

### **Immunoblotting**

Cells were lysed in cold 1X Cell Signaling Lysis Buffer (Cell Signaling) containing Complete, EDTA-free Protease Inhibitor Cocktail Tablet (Roche Diagnostics) and PhosSTOP Phosphatase Inhibitor Tablet (Roche Diagnostics), resolved by electrophoresis on 10% NuPAGE Bis-Tris Gels (Invitrogen) or 10% Tris-HCl pre-cast Ready Gels (BioRad Laboratories) and transferred to nitrocellulose membranes

(BioRad Laboratories). Blots were incubated with primary antibody to p-Syk (Y525/526) (Cell Signaling, 2711), total Syk (Santa Cruz Biotechnology, SC-1240),  $\beta$ -Actin (Abcam, ab8227-50), GAPDH (Abcam, ab22556-100) or Vinculin (Abcam, ab18058) followed by secondary antibodies anti-rabbit-HRP (Amersham #NA9340V) or anti-mouse-HRP (Amersham #NA9310V). Bound antibody was detected by chemiluminescence. For immunoprecipitation, cells were washed with cold phosphate-buffered saline and lysed in cold 1X Cell Signaling Lysis Buffer (Cell Signaling) containing Complete, EDTA-free Protease Inhibitor Cocktail Tablet (Roche Diagnostics). Two mg of each protein in lysis buffer were incubated with 2  $\mu$ g/ml anti-Syk antibody (Santa Cruz, SC-1240) for four hours at 4 °C. The immunocomplex was precipitated using 30  $\mu$ l UltraLink Immobilized Protein A/G beads (Pierce) overnight at 4 °C. The beads were then washed twice with cold 1x Cell Signaling Lysis Buffer (Cell Signaling) containing protease inhibitor, resuspended in 10  $\mu$ l of 4X SDS-sample buffer, and boiled for five minutes. The protein was then separated by electrophoresis with a 10% Tris-HCl pre-cast Ready Gel (BioRad Laboratories) and transferred to a nitrocellulose membrane (BioRad Laboratories). Blots were probed with anti-pSyk (Y525/526) (Cell Signaling #2711) and incubated with anti-rabbit-HRP (Amersham #NA9340V). Bound antibody was detected by SuperSignal West Dura Extended Duration Substrate (Pierce).

### **Xenograft Studies**

All animal studies were performed on Dana-Farber Cancer Institute IACUC approved protocols. For KG-1 xenografts, three hours prior to injection, 6 week old male NOD-SCID IL2R $\gamma$ <sup>null</sup> mice (NOG, Jackson Laboratory) were sublethally irradiated with 200 rad. 2x10<sup>6</sup> KG-1-LucNeo cells were injected via tail vein, and total body leukemia burden was assessed by bioluminescence imaging (BLI) as previously described



**(Armstrong et al., 2003)**. Animals were imaged 5 and 7 days after injection, and mice with established disease, manifested as increasing bioluminescence, were divided into cohorts that were treated with normal feed, or feed impregnated with R788 at 5 gm/kg AIN-76A rodent diet or 8 gm/kg AIN-76A rodent diet. Serial imaging was used to assess disease burden, and data plotted as the mean  $\pm$  SEM for each group. After 8 days on treatment, all mice were euthanized, and tissue collected. Spleen weights were expressed as mean  $\pm$  SEM. Significance was determined by one way ANOVA analysis with Tukey post-test to determine the significance of all pairwise comparisons.

Murine AML was induced by retroviral transduction of bone marrow with MLL-AF9 as previously described **(Stubbs et al., 2008)**. Briefly, bone marrow was harvested from a transgenic mouse with ubiquitous luciferase expression (C57BL/6:UbC6-Luc) and transduced with a retrovirus encoding MLL-AF9 (MSCV-MLL-AF9-pgkNeo). Development of leukemia was determined by BLI using the IVIS Spectrum system (Caliper Life Sciences) and by clinical scoring. To establish a cohort of mice for drug treatment studies, 30 albino co-isogenic mice (C57BL/6:Tyr<sup>C/C</sup>, Jackson Labs) were sub-lethally irradiated with 300 rads, then injected with  $10^6$  mononuclear cells isolated from the spleen of a mouse with primary AML. Mice underwent BLI weekly, and at 3 weeks post injection, animals with documented disease (increasing bioluminescence) were divided into 2 cohorts of mice with equal mean bioluminescence. The treatment group (n=10) was started on diet impregnated with R788 at 3 g/kg AIN-76A rodent diet. The control group (n=10) was kept on a normal diet. Mice underwent serial BLI at the indicated days of treatment and were euthanized after the last imaging time point for ex vivo analysis. Total body bioluminescence was quantitated using standardized regions of interest (Living Images, Caliper Life Sciences), and are expressed as mean  $\pm$  SEM.

Statistical significance for BLI data and spleen weights were calculated using Student's t-test.

For the primary human orthotopic model of AML, NOG mice were sublethally irradiated with 200 rad and then injected by tail vein injection with  $4 \times 10^5$  viable AML cells (Patient R11). Seventy days post injection, mice developed greater than 40% peripheral AML blasts as measured by FACS analysis of human specific CD45+ cells from peripheral blood. Mice were then divided into 2 cohorts with 2 animals per cohort. One group received R788 as a food product containing 5g R788/kg AIN-76 rodent diet and the second a placebo food. A NOG control mouse without human AML was included. Six days post treatment, tail vein blood was sampled and peripheral AML blasts again measured by FACS analysis of human specific CD45+ cells. At day 7, animals were euthanized and tissue collected.

### **Microarray Data**

Previously published raw microarray data (**Stegmaier et al., 2004**) is available at [http://www.broad.mit.edu/cancer/pub/GE-HTS\\_leuk](http://www.broad.mit.edu/cancer/pub/GE-HTS_leuk) or <http://www.ncbi.nlm.nih.gov/geo>

## Supplemental References

- Armstrong, S. A., Kung, A. L., Mabon, M. E., Silverman, L. B., Stam, R. W., Den Boer, M. L., Pieters, R., Kersey, J. H., Sallan, S. E., Fletcher, J. A., *et al.* (2003). Inhibition of FLT3 in MLL. Validation of a therapeutic target identified by gene expression based classification. *Cancer Cell* 3, 173-183.
- Duda, R. O., and Hart, P. E. (1973). *Pattern Classification and Scene Analysis*, (New York: John Wiley & Sons, Inc.).
- Golub, T. R., Slonim, D. K., Tamayo, P., Huard, C., Gaasenbeek, M., Mesirov, J. P., Coller, H., Loh, M. L., Downing, J. R., Caligiuri, M. A., *et al.* (1999). Molecular classification of cancer: class discovery and class prediction by gene expression monitoring. *Science* 286, 531-537.
- John, G. H., and Langley, P. (1995). Estimating Continuous Distributions in Bayesian Classifiers. In *Proceedings of the 11th Conference on Uncertainty in Artificial Intelligence*, P. Besnard, and S. Hanks, eds. (Montreal, Canada: Morgan Kaufman), pp. 338-345.
- Moffat, J., Grueneberg, D. A., Yang, X., Kim, S. Y., Kloepfer, A. M., Hinkle, G., Piqani, B., Eisenhaure, T. M., Luo, B., Grenier, J. K., *et al.* (2006). A lentiviral RNAi library for human and mouse genes applied to an arrayed viral high-content screen. *Cell* 124, 1283-1298.
- Peck, D., Crawford, E. D., Ross, K. N., Stegmaier, K., Golub, T. R., and Lamb, J. (2006). A method for high-throughput gene expression signature analysis. *Genome Biol* 7, R61.

- Rush, J., Moritz, A., Lee, K. A., Guo, A., Goss, V. L., Spek, E. J., Zhang, H., Zha, X. M., Polakiewicz, R. D., and Comb, M. J. (2005). Immunoaffinity profiling of tyrosine phosphorylation in cancer cells. *Nat Biotechnol* 23, 94-101.
- Stegmaier, K., Ross, K. N., Colavito, S. A., O'Malley, S., Stockwell, B. R., and Golub, T. R. (2004). Gene expression-based high-throughput screening(GE-HTS) and application to leukemia differentiation. *Nat Genet* 36, 257-263.
- Stubbs, M. C., Kim, Y. M., Krivtsov, A. V., Wright, R. D., Feng, Z., Agarwal, J., Kung, A. L., and Armstrong, S. A. (2008). MLL-AF9 and FLT3 cooperation in acute myelogenous leukemia: development of a model for rapid therapeutic assessment. *Leukemia* 22, 66-77.
- Vapnik, V. N. (1998). *Statistical Learning Theory*, (New York: John Wiley and Sons, Inc.).

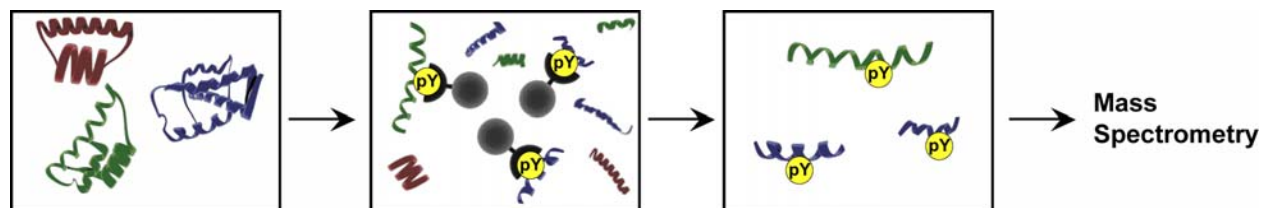


**Figure S1. A mass spectrometry approach identifies Syk as a candidate protein target of gefitinib**

Schema for Peptide-IP/LC-MS-MS. Cells were lysed, disulfide bonds reduced, and the lysates digested with trypsin and chymotrypsin, to provide complementary peptide compositions. Immunoprecipitation was performed with a cocktail of three phospho-tyrosine antibodies to enrich for phospho-tyrosine-containing peptides. The immunoprecipitation eluates were analyzed on a ThermoFisher LTQ-Orbitrap instrument which provides high resolution and mass accuracy to achieve highly specific and accurate peptide assignment. Finally, data were processed using SpectrumMill (Agilent Technologies) which not only assigns phosphopeptide identities but also enables semi-quantitation of peptide levels across different samples.

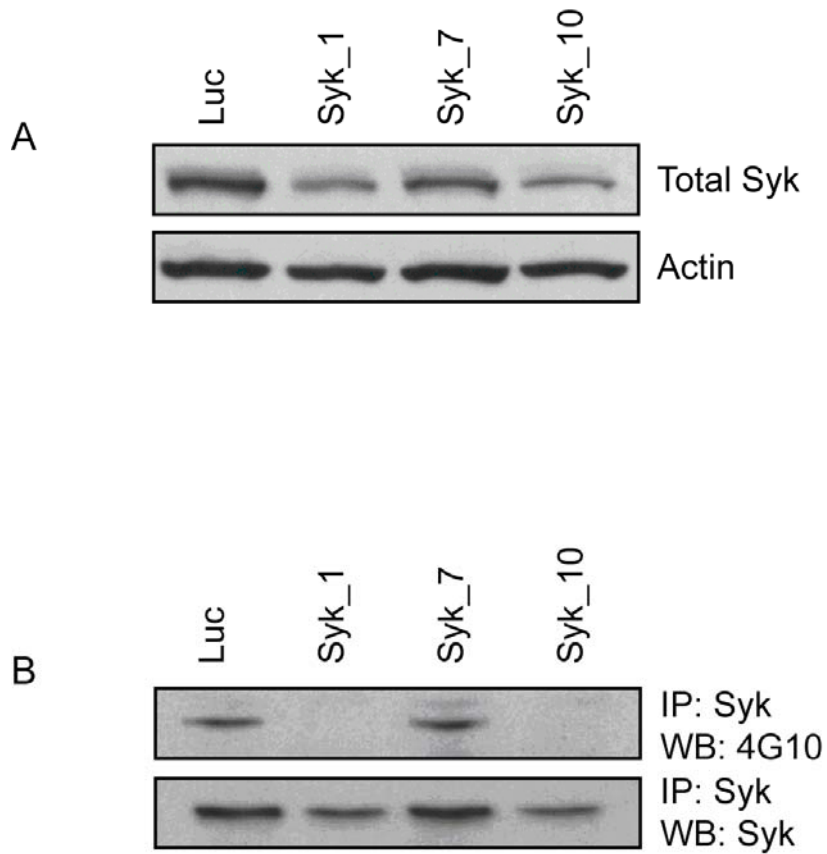


**Figure S2. Western knockdown performance of shRNAs targeting SYK**

(A) Knockdown performance of shRNAs targeting SYK compared to a Luciferase (Luc) control in MOLM-14. Total Syk protein level was evaluated at 11 days post-infection by immunoblotting. Actin is used as a loading control.

(B) Knockdown performance of shRNAs targeting SYK compared to a Luciferase (Luc) control in MOLM-14. Total Syk protein level was evaluated at 7 days post-infection by immunoprecipitation followed by immunoblotting.

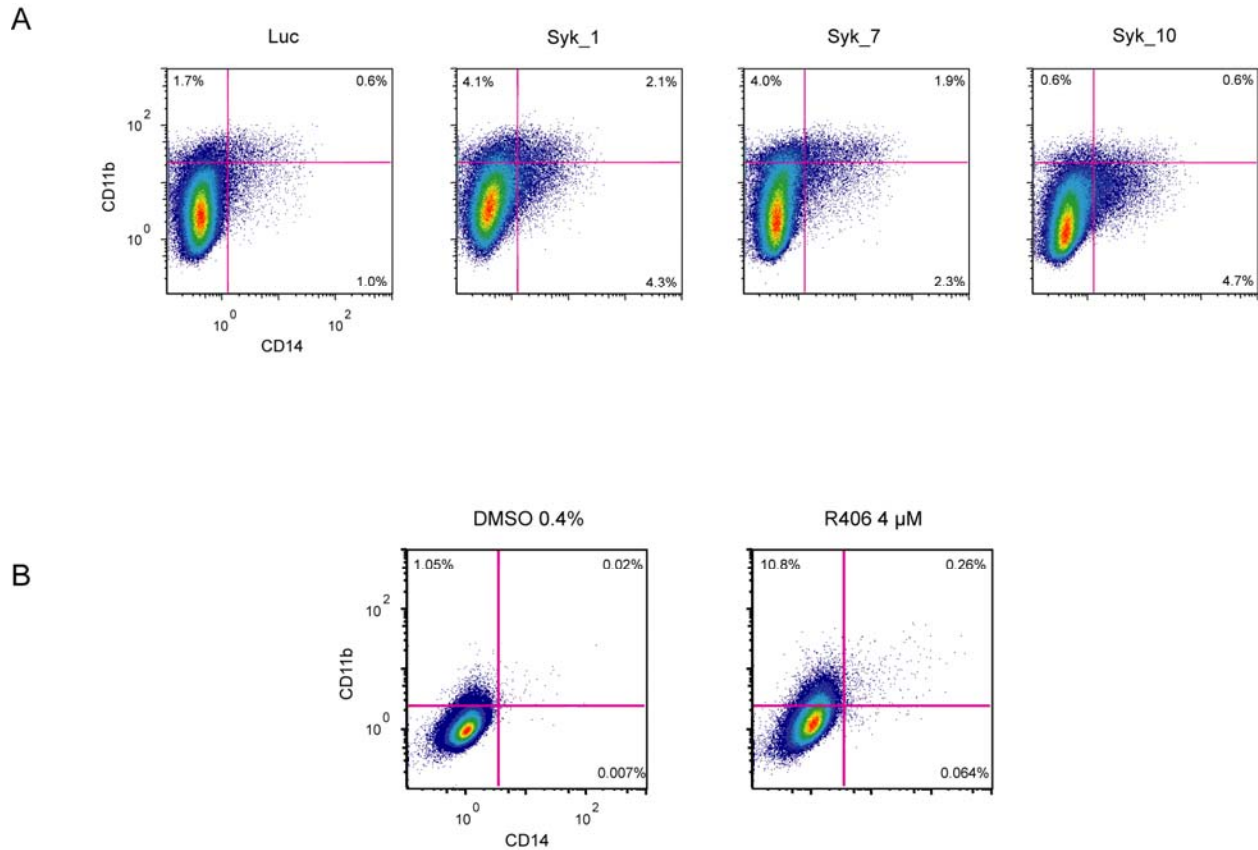
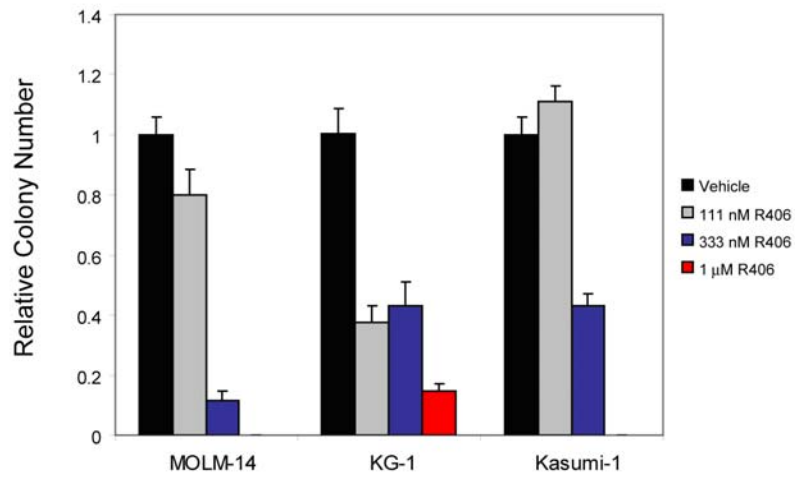


**Figure S3. SYK-directed RNAi and R406 induce CD11b and CD14 in U937 cells**

(A) Fluorescence-activated cell sorting analysis was performed with FITC and PE-labeled antibodies for CD11b and CD14, respectively. Six days post-infection with shRNAs targeting SYK, there was an increase in U937 cells positive for single stained CD11b and CD14 as well as double staining compared to a luciferase control hairpin.

(B) Fluorescence-activated cell sorting analysis was performed with FITC and PE-labeled antibodies for CD11b and CD14, respectively. U937 cells were treated for three days with vehicle or 4  $\mu$ M R406. R406 induced CD11b expression and a subtle increase in CD14 consistent with myeloid maturation.

A



B

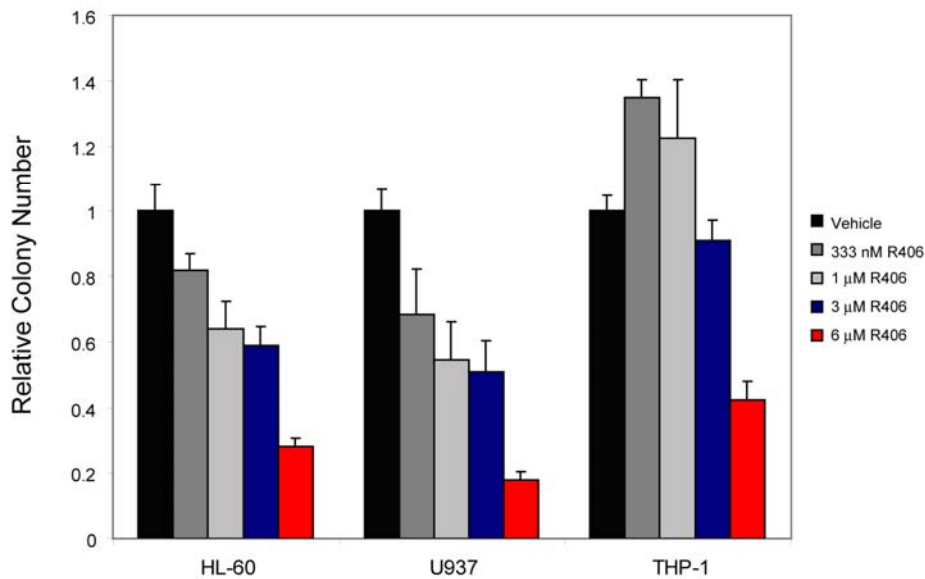


### Figure S4. R406 Impairs Colony Formation in AML Cell Lines

(A) The ability of AML cell lines (MOLM-14, KG-1 and Kasumi-1) to form colonies in methylcellulose with R406 treatment was assessed. Colonies per 4 cm<sup>2</sup> were counted in duplicate and displayed relative to control cells. Error bars depict mean ± SD.

(B) The ability of AML cell lines (HL-60, U937 and THP-1) to form colonies in methylcellulose with R406 treatment was assessed. Colonies per 4 cm<sup>2</sup> were counted in duplicate and displayed relative to control cells. Error bars depict mean ± SD.



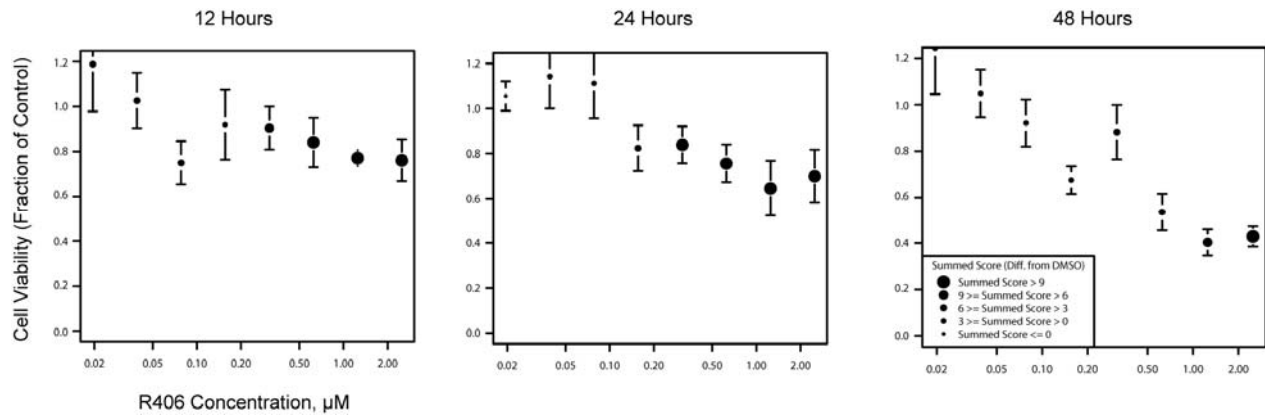


**Figure S5. Effects of Syk inhibition on viability and differentiation in KG-1**

KG-1 were treated with R406 for 12, 24, and 48 hours. Viability was measured by an ATP-based assay (y-axis). Error bars depict the mean  $\pm$  SD across 8 replicates. Gene expression is measured by the difference in Summed Score of the 32-gene differentiation signature between the R406-treated sample and the matched DMSO control. The size of each data point represents the magnitude of difference in the Summed Score where the larger the data point the more differentiated the sample is. Changes in the differentiation signature preceded the effects on viability at 12 and 24 hours. At 48 hours, R406 has effects on viability and differentiation with a dose-response.

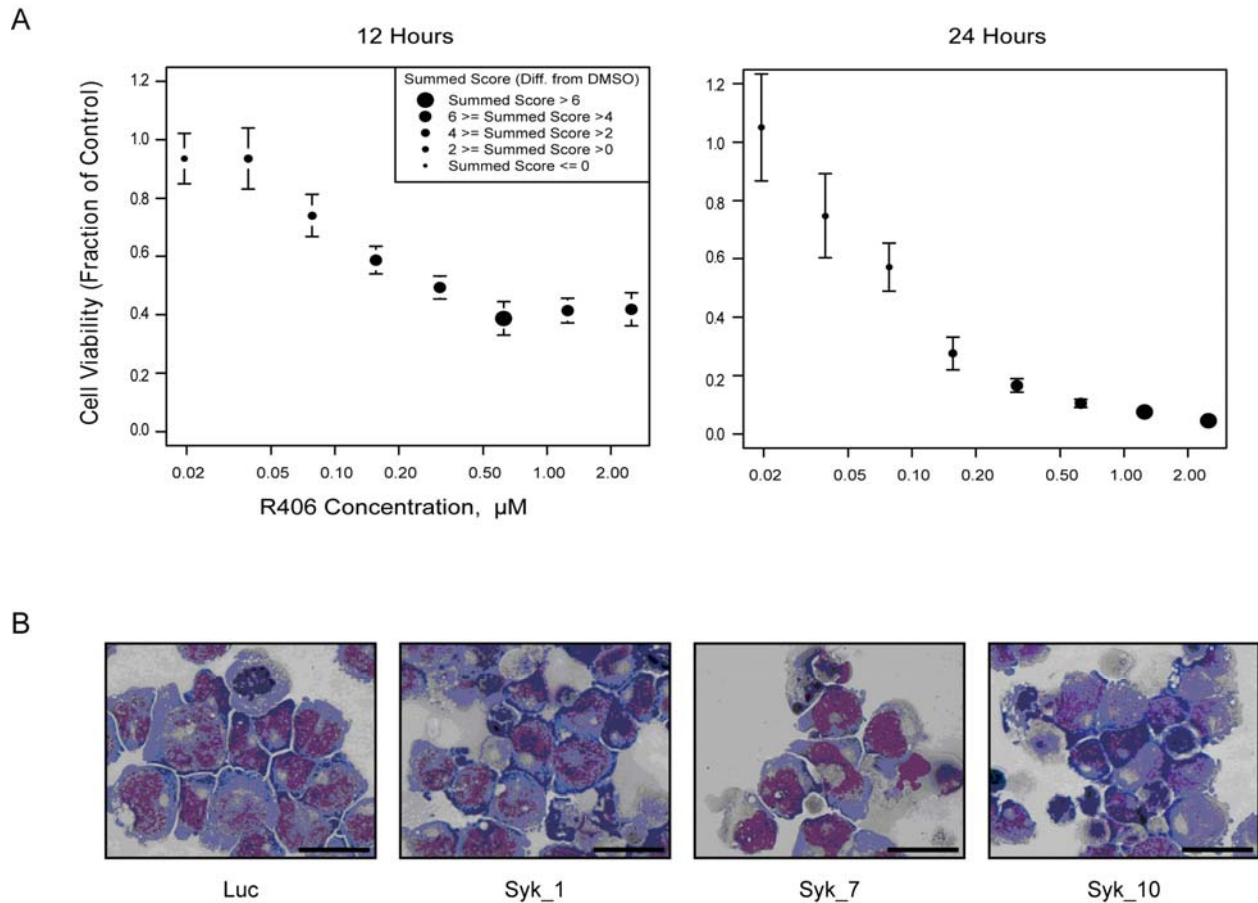


**Figure S6. Effects of Syk inhibition on viability and differentiation in MOLM-14**

(A) MOLM-14 were treated with R406 for 12 and 24 hours. Viability was measured by an ATP-based assay (y-axis). Error bars depict the mean  $\pm$  SD across 8 replicates. Gene expression is measured by the difference in Summed Score of the 32-gene differentiation signature between the R406-treated sample and the matched DMSO control. The size of each data point represents the magnitude of difference in the Summed Score where the larger the data point the more differentiated the sample is. Effects on viability were more prominent than effects on differentiation.

(B) May Grunwald Giemsa staining of MOLM-14 cells 7 days post infection with shRNA targeting *SYK* versus a luciferase shRNA control demonstrate evidence of cell death with pyknotic nuclei. Images were acquired with an Olympus BX41 microscope, 1000x magnification under oil, and Qcapture software. The scale bar equals 25  $\mu$ M.

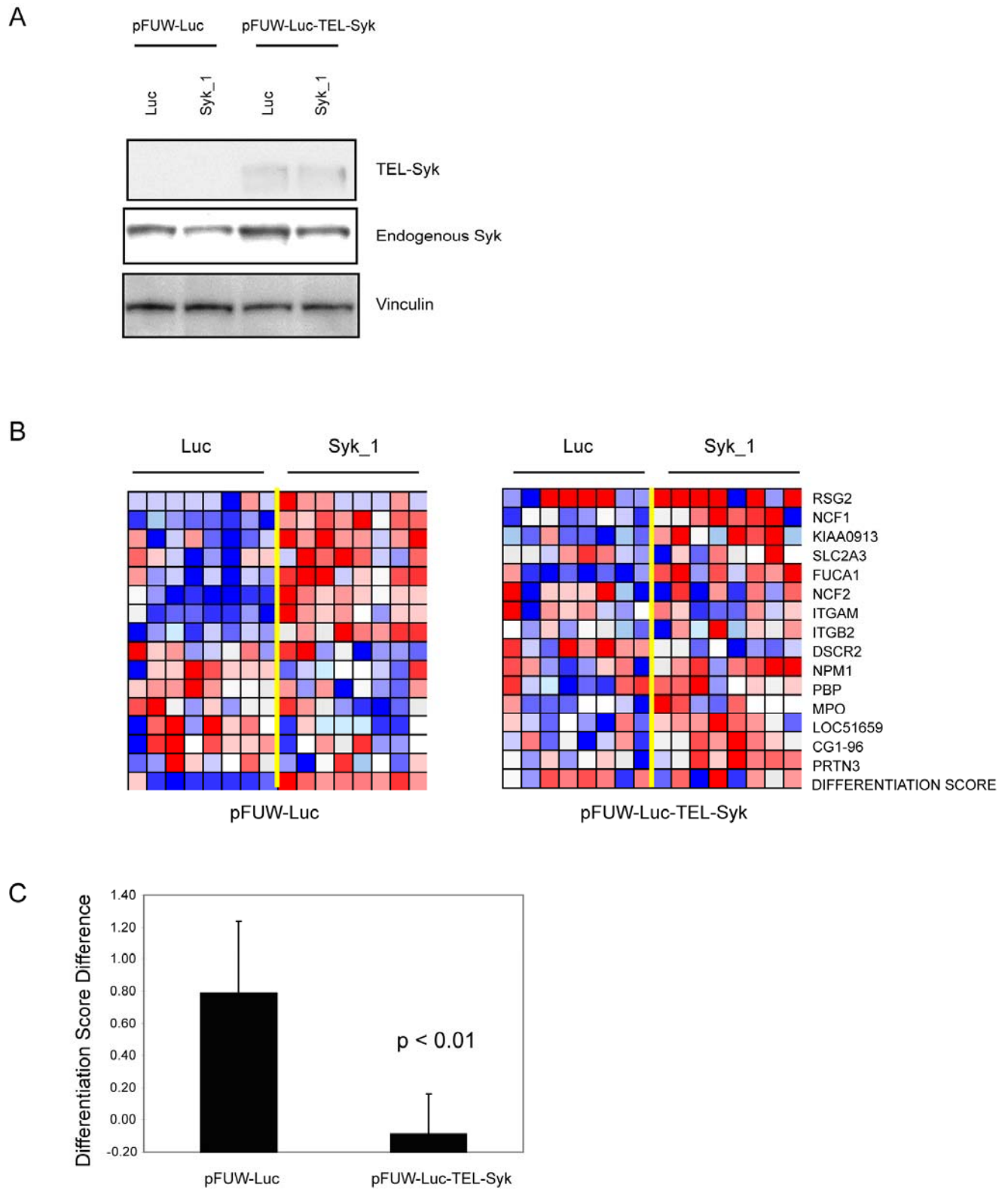


**Figure S7. TEL-Syk rescues the Syk\_1 shRNA differentiation effect in MOLM-14**

(A) TEL-Syk, immune to Syk\_1 shRNA, was expressed in MOLM-14 cells (pFUW-Luc-TEL-Syk). Knockdown performance of shRNA targeting SYK (Syk\_1) was then compared to a Luciferase (Luc) control hairpin in the TEL-Syk expressors versus control

(pFUW-Luc) cells. Total protein was evaluated three days post-infection. Vinculin is used as a loading control.

(B) As in A above, MOLM-14 cells ectopically expressing non-targetable TEL-Syk versus a control were transduced with Syk\_1 shRNA versus Luc shRNA and a differentiation signature measured 7 days after infection in 8 replicates. Fifteen of the 32 signature genes changed in the appropriate direction in the pFUW-Luc control (8 upregulated and 7 downregulated genes) with knockdown of Syk. This differentiation signature was significantly attenuated in the TEL-Syk condition.

(C) A Differentiation Score (Summed Score) was calculated for each condition pFUW-Luc (Luc shRNA versus Syk\_1 shRNA) and pFUW-Luc-TEL-Syk (Luc shRNA versus Syk\_1 shRNA) for the above 15 marker genes. The difference between the Syk\_1 score and the Luc score was then determined. The induction of the differentiation signature was significantly attenuated in the TEL-Syk rescue with  $p < 0.01$  by t-test. Error bars depict the mean  $\pm$  SD across the differences between the 8 Syk\_1 shRNA replicates and the 8 Luc shRNA replicates.

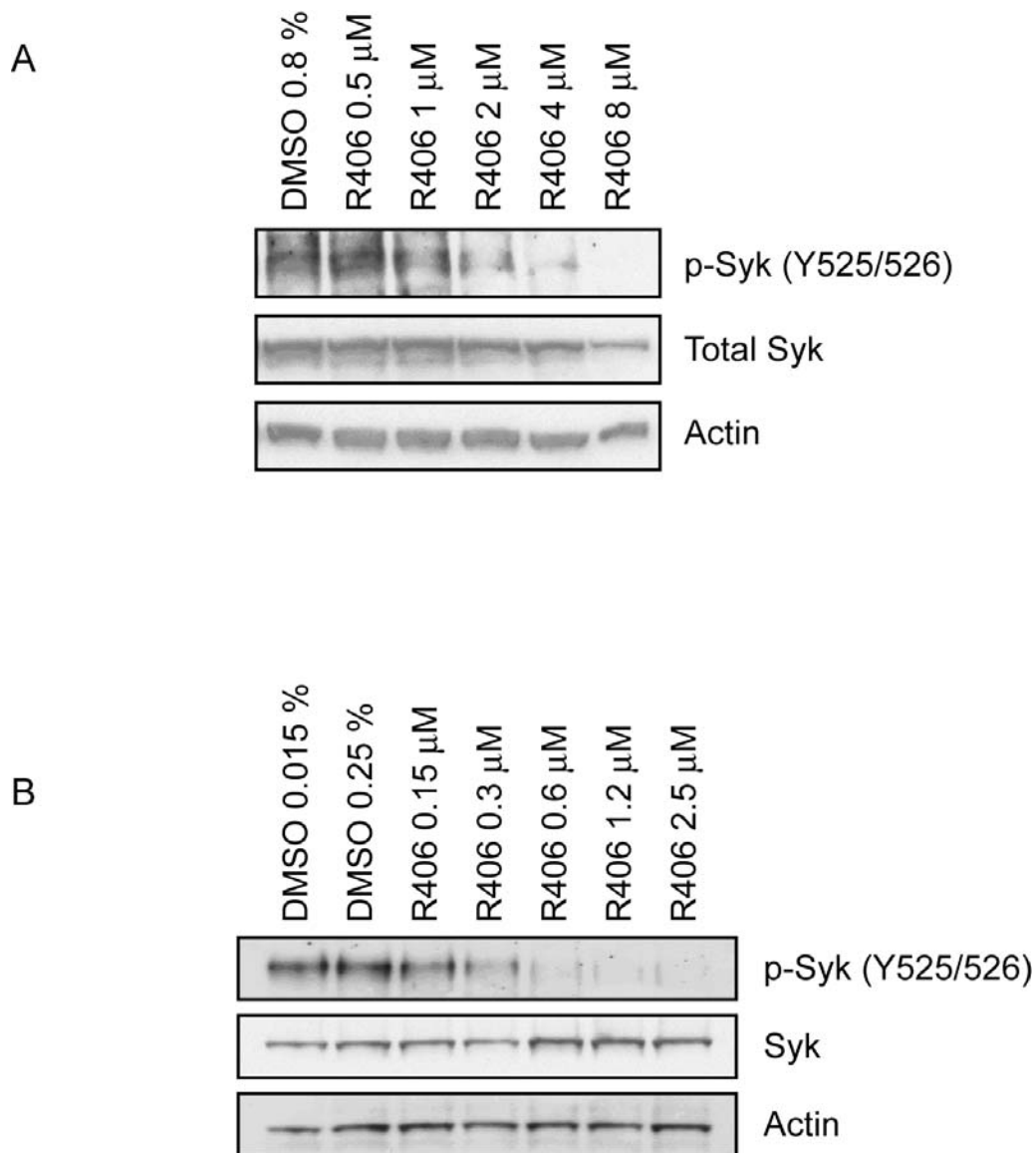


**Figure S8. Dose-response of p-Syk (Y525/526) with R406 treatment**

(A) U937 cells were treated with DMSO or R406 for 24 hours and blotted with an antibody to p-Syk (Y525/526), total Syk, or actin. There is a tight correlation between loss of p-Syk and the Differentiation Score (Figure 3B).

(B) KG-1 cells were treated with DMSO or R406 for 24 hours and blotted with an antibody to p-Syk (Y525/526), total Syk, or actin. There is a tight correlation between loss of p-Syk and the Differentiation Score (Figure 4F).

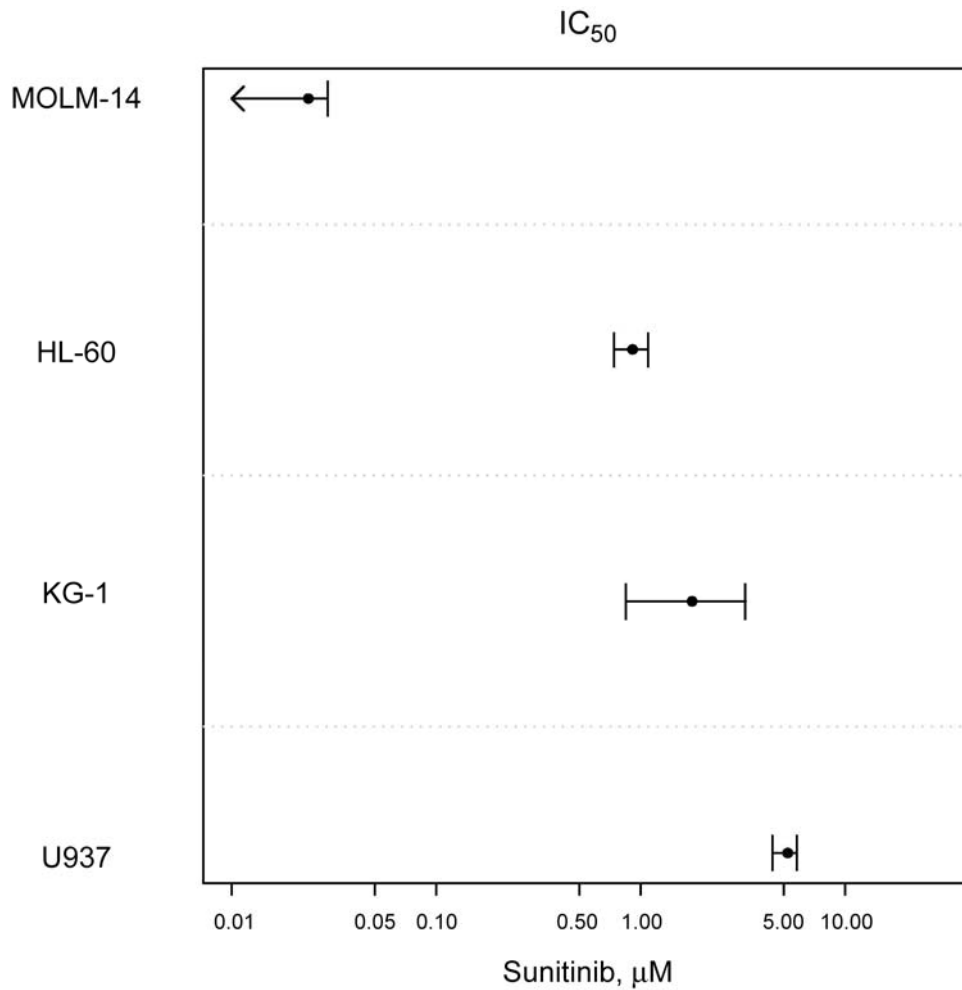


**Figure S9. Sunitinib does not affect FLT-3 wild-type AML at FLT-3 inhibitory doses**

The AML cell lines MOLM-14, KG-1, HL-60, and U937 were treated for three days with sunitinib in a 2-fold dilution from 20  $\mu M$  to 0.02  $\mu M$  and viability was measured with an ATP-based assay. The  $IC_{50}$  for each cell line is reported. Only the FLT-3 mutant cell line, MOLM-14, responded at doses that inhibit FLT-3. Range bars represent the upper and lower 0.95 confidence bounds for the SEM for the 6 sunitinib replicates relative to the 6 control replicates.

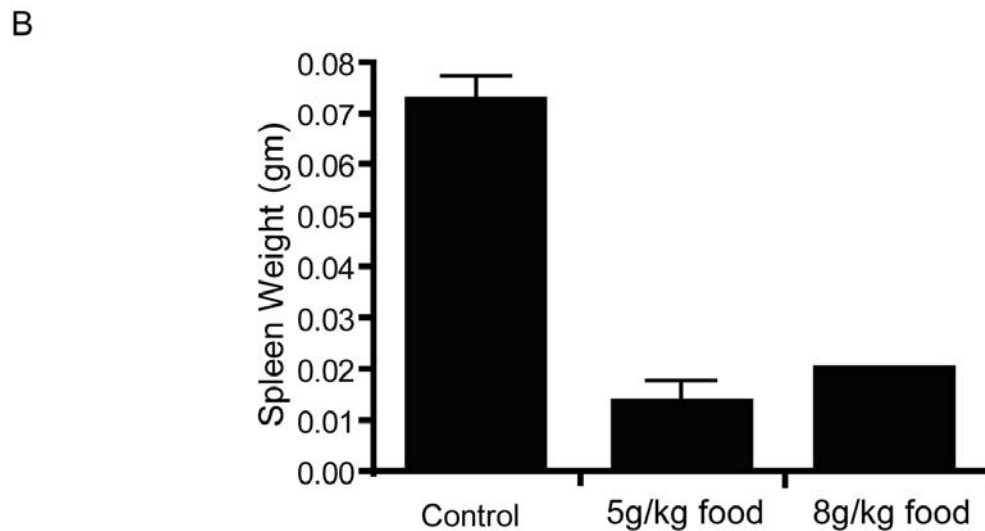
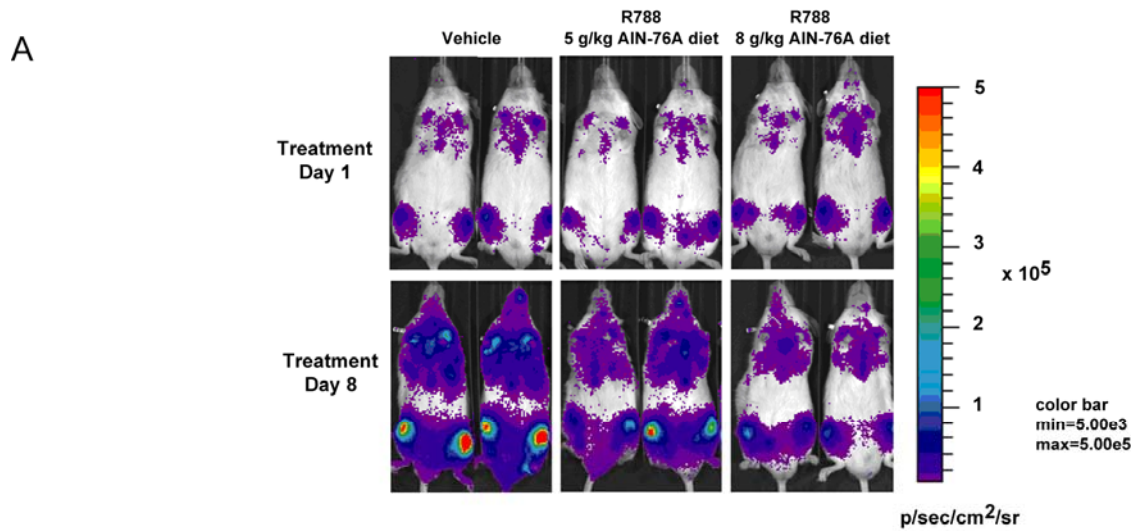


**Figure S10. Effects of R788 in a KG-1 xenograft**

(A) KG-1 luciferase positive xenografts were established in NOG mice with tumor burden monitored by bioluminescence. Mice were treated with placebo (n=4), food impregnated with R788 at 5g/kg AIN-76A food (n=5), and food impregnated with 8g/kg AIN-76A food (n=3) for 8 days. Mice treated with R788 have a significant decrease in tumor burden as measured by bioluminescence.

(B) By Tukey's Multiple Comparison Test, R788-treated animals had spleen sizes statistically smaller than control-treated animals with  $p < 0.001$ . The error bars denote SEM.

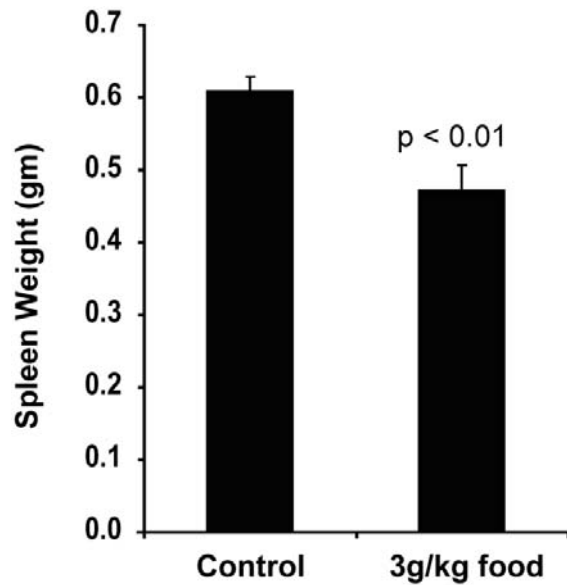


**Figure S11. Effects of R788 in a syngeneic MLL-AF9 mouse model of AML**

A syngeneic mouse model of MLL-AF9 AML was established and mice treated with either control food (N=10) or food containing R788 at 3g/kg AIN-76A food (N=10) for 8 days. Statistical significance for spleen weight was calculated using Student's t-test. The error bars denote SEM.



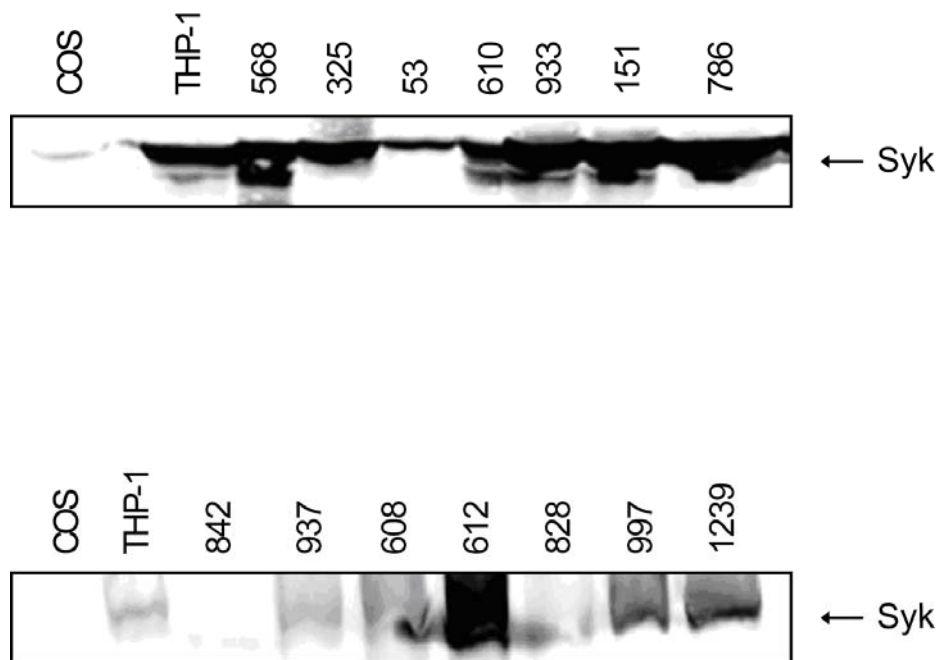


**Figure S12. Primary patient AML blasts express Syk protein**

Immunoblots of primary patient AML blasts blotted with an antibody to total Syk. COS cells were included as a negative control for Syk expression and the AML cell line THP-1 as a positive control. Individual patient samples are noted by a unique number. Thirteen of the 14 samples express Syk protein.

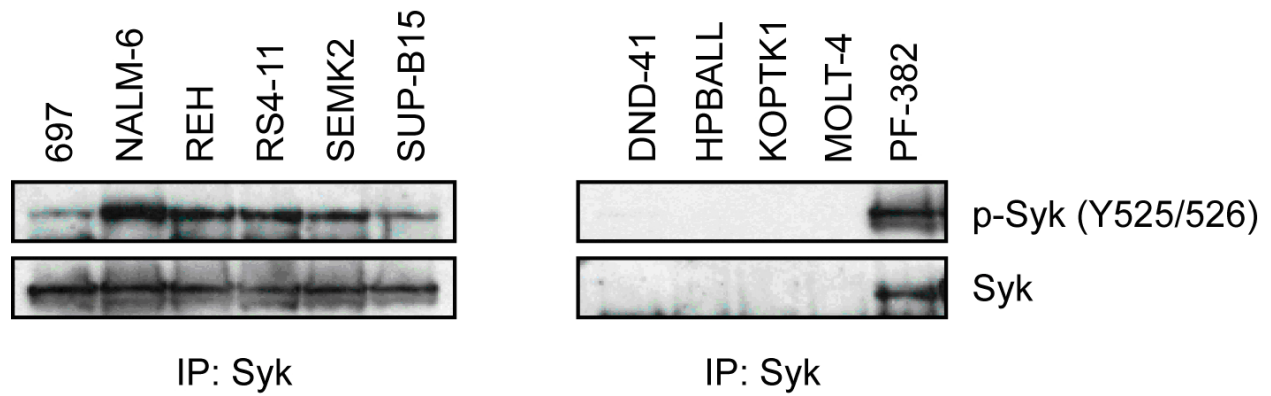


**Figure S13. Syk protein expression and phosphorylation at Y525/526 in ALL cell lines**

Pre-B ALL (left) and T-ALL (right) cell lines were immunoprecipitated with total Syk antibody and then blotted for p-Syk (Y525/526) and total Syk.

## Table S1. Phosphorylation sites mapped in pTyr immunoprecipitated peptides from HL-60 cells treated with gefitinib vs DMSO

### Terms used in Table S1:

Columns	
Z	Precursor charge of the peptide.
Score	Score from the interpretation of the peptide's MS/MS spectrum.
SPI	Scored percent intensity from the interpretation of the peptide's MS/MS spectrum.
Site Ambiguity	Possible indistinguishable positions of the phosphorylated residue(s) if the fragment ion series observed in the MS/MS spectrum are incomplete.
Sequence	y: phospho Tyr, s: phospho Ser, t: phospho Thr, m: oxidized Met, n: deamidated Asn, q: pyro Glu from Gln

For simplicity, when a phosphorylation site was observed in multiple forms only the highest scoring peptide or the one with the least ambiguity in phosphosite assignment is listed in the table. Multiple forms of detecting a particular phosphorylation site can arise from multiple precursor charge states, different peptides resulting from trypsin/chymotrypsin, missed cleavage by the enzyme, and variable modification of certain amino acids in the peptide due to the isolation procedure (oxidation of methionine, deamidation of asparagine, pyroglutamic acid formation at peptide N-terminal glutamines, and carbamylation of peptide N-termini by urea).

DMSO		Gefitinib		m/z	Phosphorylation	Site	Sequence	HUGO	NCBI	Note	HUGO	Protein
z	Score	z	Score	Obs. (Da)	Site(s)	Ambiguity		Symbol	gi		Name	Name
2	13.06	815	2	12.14	723.304	Y1189	(R)DIVETDYR(K)	INSR	4567884	Kinase-Tyr	insulin receptor	INSR TK:InsR insulin receptor
2	20.86	946	2	20.65	1103.510	Y223	ok (K)VVALLDYMFMNANDLQR(K)	BTX	4567377	Kinase-Tyr	Brunon agammaglobulinemia tyrosine kinase	BTX TK:Te Brunon agammaglobulinemia tyrosine kinase
3	17.00	885	3	17.00	966.445	Y323	ok (R)QESTVSNFYEPALPWAADKGPQR(E)	SVK	2136153	Kinase-Tyr	spleen tyrosine kinase	SVK TK:Sk spleen tyrosine kinase
2	14.18	913	2	15.81	764.323	Y537	ok (F)TATEPQGPEN(L)	YES1	4885661	Kinase-Tyr	v-yes-1 Yamaguchi sarcoma viral oncogene homolog 1	FYN TK:Src FYN oncogene related to SRC, FGR, YES
3	23.22	953	3	23.22	1173.850	Y508	ok (K)AERPTFDYLGSLDDFYATEGGYQQQ(F)	LYN	4505055	Kinase-Tyr	v-yes-1 Yamaguchi sarcoma viral related oncogene homolog	FGR TK:Src Gardner-Rasheed feline sarcoma viral (v-fgr) oncogene homolog
3	20.45	864	3	20.45	665.769	Y508	ok (Y)TATEGQQQ(F)	LYN	4505055	Kinase-Tyr	v-yes-1 Yamaguchi sarcoma viral related oncogene homolog	LYN TK:Src v-yes-1 Yamaguchi sarcoma viral related oncogene homolog
2	14.63	803	2	11.37	645.274	Y411	ok (K)TETSASHPCPVVPDPTSTKPGNSHNSNTPGIR(E)	HCK	3078629	Kinase-Tyr	hemopoietic cell kinase	HCK TK:Src hemopoietic cell kinase
2	14.63	803	2	11.37	645.274	Y411	ok (R)VEDNYTAR(E)	HCK	3078629	Kinase-Tyr	hemopoietic cell kinase	HCK TK:Src hemopoietic cell kinase
2	13.71	882	2	12.34	647.779	Y359	ok (K)TVCTYLGSR(Y)	HPK3	2949069	Kinase-Ser/Thr	homodomain interacting protein kinase 3	HPK3 CMGC:DYRK homodomain interacting protein kinase 3
2	15.56	774	2	14.89	632.774	Y351	ok (K)LVCSFGASHADNDITPYLVS(R)	PRPF4B	1799595	Kinase-Ser/Thr	PRPF4 pre-mRNA processing factor 4 homolog B (yeast)	PRPF4B CMGC:DYRK PRPF4 pre-mRNA processing factor 4 homolog B (yeast)
3	21.27	951	3	21.29	854.046	Y849	ok (R)YVQGR(F)	DYRK1A	1676752	Kinase-Ser/Thr	dual-specificity tyrosine-(Y)-phosphorylation regulated kinase 1A	DYRK1A CMGC:DYRK dual-specificity tyrosine-(Y)-phosphorylation regulated kinase 1A
2	16.49	957	2	16.53	681.283	Y279	ok (R)GEPNVISCS(R)	MAPK10	4506081	Kinase-Ser/Thr	mitogen-activated protein kinase 10	MAPK10 CMGC:MAPK mitogen-activated protein kinase 10
2	15.52	858	2	14.78	976.383	T183	Y183Y ok (R)TACTNFMMFPV(VTR(Y))	MAPK9	1170558	Kinase-Ser/Thr	mitogen-activated protein kinase 9	MAPK9 CMGC:MAPK mitogen-activated protein kinase 9
3	16.07	814	3	13.56	751.340	Y204	ok (R)ADPEHDHTGFLTEVATR(W)	MAPK3	38257141	Kinase-Ser/Thr	mitogen-activated protein kinase 3	MAPK3 CMGC:MAPK mitogen-activated protein kinase 3
3	16.87	871	3	16.87	777.995	T201	Y204Y ok (R)ADPEHDHTGFLTEVATR(W)	MAPK3	38257141	Kinase-Ser/Thr	mitogen-activated protein kinase 3	MAPK3 CMGC:MAPK mitogen-activated protein kinase 3
2	17.39	879	2	17.10	808.808	T183	Y183Y ok (R)QADEMGTGV(VTR(W))	MAPK12	2851522	Kinase-Ser/Thr	mitogen-activated protein kinase 12	MAPK12 CMGC:MAPK mitogen-activated protein kinase 12
2	16.84	974	2	16.82	788.312	Y122	ok (R)HTDDEMTGV(VTR(W))	MAPK14	4503069	Kinase-Ser/Thr	mitogen-activated protein kinase 14	MAPK14 CMGC:MAPK mitogen-activated protein kinase 14
3	18.42	876	3	18.19	828.295	T180	Y182Y ok (R)HTDDEMTGV(VTR(W))	MAPK14	4503069	Kinase-Ser/Thr	mitogen-activated protein kinase 14	MAPK14 CMGC:MAPK mitogen-activated protein kinase 14
3	9.18	569	3	14.42	711.996	Y175Y	ok (R)VADPDHHTGFLTEVATR(W)	MAPK1	23879	Kinase-Ser/Thr	mitogen-activated protein kinase 1	MAPK1 CMGC:MAPK mitogen-activated protein kinase 1
2	17.66	894	2	17.72	868.933	Y15Y	ok (Y)TKIKGEGTGVV(YK)	CDC2	4502709	Kinase-Ser/Thr	cell division cycle 2, G1 to S and G2 to M	CDC2 CMGC:CDK cell division cycle 2, G1 to S and G2 to M
2	16.73	915	2	15.71	906.914	T14	Y15Y ok (Y)TKIKGEGTGVV(YK)	CDC2	4502709	Kinase-Ser/Thr	cell division cycle 2, G1 to S and G2 to M	CDC2 CMGC:CDK cell division cycle 2, G1 to S and G2 to M
2	16.94	908	2	17.52	654.798	Y15Y	ok (K)IGETGVV(YK)	CDC2	4502709	Kinase-Ser/Thr	cell division cycle 2, G1 to S and G2 to M	CDC2 CMGC:CDK cell division cycle 2, G1 to S and G2 to M
2	13.00	865	2	13.06	694.782	T14	Y15Y ok (K)IGETGVV(YK)	CDC2	4502709	Kinase-Ser/Thr	cell division cycle 2, G1 to S and G2 to M	CDC2 CMGC:CDK cell division cycle 2, G1 to S and G2 to M
2	15.40	847	2	15.12	633.296	Y19Y	ok (K)IGETGVV(YKGRH)	CDC2	4502709	Kinase-Ser/Thr	cell division cycle 2, G1 to S and G2 to M	CDC2 CMGC:CDK cell division cycle 2, G1 to S and G2 to M
2	9.34	441	2	9.34	739.857	Y19Y	ok (K)IGETGVV(YK)	CDK3	457439	Kinase-Ser/Thr	cyclin-dependent kinase 3	CDK3 CMGC:CDK cyclin-dependent kinase 3
2	16.94	904	2	17.52	654.798	Y15Y	ok (K)IGETGVV(YK)	CDK3	457439	Kinase-Ser/Thr	cyclin-dependent kinase 3	CDK3 CMGC:CDK cyclin-dependent kinase 3
2	13.00	866	2	13.06	694.782	T14	Y15Y ok (K)IGETGVV(YK)	CDK3	457439	Kinase-Ser/Thr	cyclin-dependent kinase 3	CDK3 CMGC:CDK cyclin-dependent kinase 3
2	8.68	405	2	10.08	675.428	Y15Y	ok (F)KQVKEGEGTGVV(YK)	CDK3	457439	Kinase-Ser/Thr	cyclin-dependent kinase 3	CDK3 CMGC:CDK cyclin-dependent kinase 3
2	11.96	886	2	11.96	915.413	T14	Y15Y ok (F)KQVKEGEGTGVV(YK)	CDK3	457439	Kinase-Ser/Thr	cyclin-dependent kinase 3	CDK3 CMGC:CDK cyclin-dependent kinase 3
2	15.40	847	2	15.12	633.296	Y19Y	ok (K)IGETGVV(YK)	CDK3	457439	Kinase-Ser/Thr	cyclin-dependent kinase 3	CDK3 CMGC:CDK cyclin-dependent kinase 3
2	19.39	981	2	20.00	769.833	Y7Y	ok (-)TNLSEQADV(R)-	CPY03	3	Control Peptide	Control Peptide 3 Pre-SepPak	Control_CPP-Pre-SepPak NEP 21b
2	12.48	707	2	12.07	666.833	Y5Y	ok (-)PFVQATL(SN)-	CPY01	1	Control Peptide	Control Peptide 1 Pre-SepPak	Control_CPP-Pre-SepPak Mepin receptor precursor Anaspep 24441
2	13.63	787	2	16.38	606.770	Y4Y	ok (-)JTHYGLS(LPEK)-	CPY05	5	Control Peptide	Control Peptide 5 Pre-IP	Control_CPP-Pre-IP Myelin basic protein S Q8E mutant, NEP 13
2	12.56	816	2	12.58	563.758	Y4Y	ok (-)DRVYHP(F)-	CPY02	2	Control Peptide	Control Peptide 2 Pre-IP	Control_CPP-Pre-IP Angiotensin II substrate Anaspep 24520
3	15.89	821	3	19.40	723.339	Y179Y	179.80 ok (R)RHPFYAPPELLYAN(KY)	B5A	1351907	Contaminant	bovine serum albumin	bovine serum albumin
2	19.67	842	2	18.20	509.259	Y142Y	ok (K)RYEQLPEVQ(K)	ALMS1	20067381	Alstrom syndrome 1	ALMS1 protein	ALMS1 protein
3	13.68	796	3	12.00	785.370	Y97Y	ok (K)REPEALAAV(NK)	ITNS2	2232585	intersectin 2	intersectin 2 isoform 1	intersectin 2 isoform 1
3	21.31	974	3	21.07	1061.848	Y98Y	986.87 ok (K)NSPNNPYYVLEGGVPHOLLPPESPAPR(A)	INPPL1	4755142	inositol polyphosphate phosphatase-like 1	inositol polyphosphate phosphatase-like 1	inositol polyphosphate phosphatase-like 1
2	6.99	578	2	6.89	972.125	Y542Y	ok (K)EQPLDEELKDAFQNAYLELGLGER(V)	ATP1A1	21361181	ATPase, Na+/K+ transporting, alpha 1 polypeptide	ATPase, Na+/K+ transporting, alpha 1 polypeptide	Na+/K+-ATPase alpha 1 subunit isoform a proprotein
3	9.95	803	3	10.74	530.247	Y260Y	ok (R)GIVYTGDR(T)	ATP1A1	21361181	ATPase, Na+/K+ transporting, alpha 1 polypeptide	ATPase, Na+/K+ transporting, alpha 1 polypeptide	Na+/K+-ATPase alpha 1 subunit isoform a proprotein
3	14.40	869	3	14.40	869.420	Y580Y	ok (R)FTGHGPAJLR(LNR(W))	TMEM16D	3020318	transmembrane protein 16D	transmembrane protein 16D	transmembrane protein 16D
3	10.74	888	3	10.74	486.265	Y242Y	ok (R)WLAJENK(LR)	BCAS3	10438048	breast carcinoma amplified sequence 3	BCAS3	Breast carcinoma amplified sequence 3 (GAOB1) (Maab1) protein
2	21.13	902	2	9.10	801.765	Y674Y	ok (K)KPPSSANAYSLAARLPV(PVK(L))	CBL	115865	Syk Pathway	Cas-Bi-M (murine) ectopic retroviral transforming sequence	CBL E3 ubiquitin protein ligase (Signal transduction protein CBL) (Proto-oncogene c-CBL)
2	20.02	931	2	19.95	839.727	N112	Y102Y ok (R)TLRSYEGMTELGAEVFR(V)	CBL	115865	Syk Pathway	Cas-Bi-M (murine) ectopic retroviral transforming sequence	CBL E3 ubiquitin protein ligase (Signal transduction protein CBL) (Proto-oncogene c-CBL)
2	21.13	902	2	9.10	801.765	Y674Y	ok (R)VGVWFYANVEEDYSEY(C)-	VAV1	7108367	Syk Pathway	vav 1 oncogene	vav 1 oncogene
2	20.02	931	2	19.95	994.939	Y789Y	ok (K)VVQYEDAFSDYANFK(-)	PTPRK	4506303	protein tyrosine phosphatase, receptor type, A	protein tyrosine phosphatase, receptor type, A isoform 1 precursor	protein tyrosine phosphatase, receptor type, A isoform 1 precursor
2	12.38	788	2	12.60	915.413	Y20Y	ok (R)SFSNLSFGGEP(LS)TR(F)	PTPRC	4507457	protein tyrosine phosphatase, receptor type, C	protein tyrosine phosphatase, receptor type, C isoform 1 precursor	protein tyrosine phosphatase, receptor type, C isoform 1 precursor
2	13.52	743	2	13.52	1000.958	Y686Y	ok (K)VVQDFDFDSDYANFK(-)	PTPRP	5729993	protein tyrosine phosphatase, receptor type, E	protein tyrosine phosphatase, receptor type, E isoform 1 precursor	protein tyrosine phosphatase, receptor type, E isoform 1 precursor
3	13.15	794	3	12.54	830.340	Y379Y	ok (R)KQDDDDDDYFLELDFGQ(K)	C1orf21	56204160	chromosome 1 open reading frame 38	chromosome 1 open reading frame 38	chromosome 1 open reading frame 38
2	10.9	590	2	9.20	541.707	Y124Y	ok (Y)SEEEKV(FI)	LCPI	4504965	lymphocyte cytosolic protein 1 (L-plastin)	lymphocyte cytosolic protein 1 (L-plastin)	L-plastin
2	15.20	849	2	15.20	1120.993	Y28Y	ok (K)QVTDGNGV(SFNLNDFK(A))	LCPI	4504965	lymphocyte cytosolic protein 1 (L-plastin)	lymphocyte cytosolic protein 1 (L-plastin)	L-plastin
3	21.33	973	3	14.74	701.667	Y275Y	ok (K)NMKEQIQEYSQIQSK(K)	TKT	4507521	transketolase (Wernicke-Korsakoff syndrome)	transketolase variant	transketolase variant
3	13.90	766	3	13.90	993.140	Y250Y	250.51 ok (K)TGASVYGEQTHYATNGESAVVQLPK(N)	EIF2A	15009229	Eukaryotic translation initiation factor 2A	Eukaryotic translation initiation factor 2A	CD402
3	16.97	725	3	11.96	796.860	Y566Y	ok (K)HKHEDVNHHT(K)	PTPN6	18104991	protein tyrosine phosphatase, non-receptor type 6	protein tyrosine phosphatase, non-receptor type 6 isoform 2	protein tyrosine phosphatase, non-receptor type 6 isoform 2
2	14.11	772	2	15.29	988.440	Y428Y	ok (R)ELFDDPSVNVNQLK(A)	SHC1	55690113	SHC (Src homology 2 domain containing) transforming protein 1	SHC1 protein	SHC1 protein
2	16.81	938	2	11.97	954.907	Y180Y	ok (L)LTGPEVHPDITVSDW(S)	CORO1A	5902134	coronin, actin binding protein, 1A	coronin, actin binding protein, 1A	coronin, actin binding protein, 1A
2	11.97	870	2	11.97	544.249	Y271Y	ok (L)IINDQLY(L)	TBCE	4507375	tubulin-specific chaperone e	tubulin-specific chaperone e	beta-tubulin cofactor E
2	23.50	1000	2	21.90	945.962	Y287Y	ok (K)LYDFIEDQGLAEV(R)	CCT2	4545803	chaperonin containing TCP1, subunit 2 (beta)	chaperonin containing TCP1, subunit 2 (beta)	chaperonin containing TCP1, subunit 2
2	10.98	763	2	10.98	959.455	Y303Y	ok (K)LYDFIEDQGLAEV(R)	WAS	12804207	Wiskott-Aldrich syndrome (eczema-thrombocytopenia)	WAS protein	WAS protein
2	7.26	680	2	9.93	697.858	Y141Y	ok (R)EHALLAYTLGV(K)	TEAD3	60552216	TEA domain family member 3	TEA domain family member 3	TEAD3 protein
2	11.15	537	2	7.76	600.787	Y29Y	ok (K)STTGHLYK(C)	EEF1A2	4503475	eukaryotic translation elongation factor 1 alpha 2	eukaryotic translation elongation factor 1 alpha 2	eukaryotic translation elongation factor 1 alpha 2
2	16.44	852	2	15.96	600.787	Y29Y	ok (R)SAAEAPLYSK(V)	EEF1A2	4503475	eukaryotic translation elongation factor 1 alpha 2	eukaryotic translation elongation factor 1 alpha 2	eukaryotic translation elongation factor 1 alpha 2
2	19.88	936	2	16.75	942.978	Y44Y	ok (R)IAVPSGASTGYALELR(D)	PTPN18	18375655	protein tyrosine phosphatase, non-receptor type 18 (brain-derived)	protein tyrosine phosphatase, non-receptor type 18	protein tyrosine phosphatase, non-receptor type 18
3	15.89	813	3	15.89	1030.141	Y317Y	ok (R)EEDFLTEESAMVSSVNRPGQLV(NK(S))	ENOC2	5803011	enolase 2 (gamma, neuronal)	enolase 2 (gamma, neuronal)	enolase 2 (gamma, neuronal)
2	15.58	788	2	13.47	761.319	Y359Y	ok (R)SFSNLSFGGEP(LS)TR(F)	PAG1	6068957	phosphoprotein associated with glycosphingolipid microdomains 1	phosphoprotein associated with glycosphingolipid microdomains 1	Phosphoprotein associated with glycosphingolipid microdomains 1
3	19.05	881	3	19.03	1088.534	Y151Y	ok (R)ITGMSDGGVTHVTPVYEGYALHPLR(L)	PHG2	34192185	pyruvate dehydrogenase (lipoteamide) alpha 2	pyruvate dehydrogenase (lipoteamide) alpha 2	pyruvate dehydrogenase (lipoteamide) alpha 2
3	11.63	856	3	11.63	836.792	Y87Y	ok (L)KGLLSPVLAAYAGNRSRLV(L)	PTGDR	28486969	prostaglandin D2 receptor (DP)	prostaglandin D2 receptor (DP)	prostaglandin D2 receptor (DP)
2	10.35	718	2	19.75	1343.513	Y316Y	ok (L)KEQYEEVGVSDVEEGEEGEEY(-)	TUB1B	18204869	tubulin, alpha 1b	tubulin, alpha 1b	K-ALPHA-1 protein
2	15.45	845	2	12.34	670.830	Y24Y	ok (K)QDLYNLK(E)	LPHA	5031857	lactate dehydrogenase A	lactate dehydrogenase A variant	lactate dehydrogenase A variant
3	13.75	719	3	13.75	867.414	Y180Y	ok (R)KTPQGPPEYSDTOPFSLQSTAK(H)	BNPT1	17389533	3'(2', 5'-bisphosphate nucleotidase 1	BNPT1 protein	BNPT1 protein
2	13.10	891	2	12.11	595.318	Y12Y	ok (R)IAJELLP(E)	RPLP0	4506667	ribosomal protein, large, P0	ribosomal protein P0 variant	ribosomal protein P0 variant
3	13.80	732	3	16.34	624.265	Y140Y	ok (K)HELQANQVEEKDR(C)	CDV3	13938400	CDV3 homolog	CDV3 homolog	H41 protein
2	14.68	769	2	14.67	709.301	Y89Y	ok (R)YALYDATYETK(E)	RPS10	4506679	ribosomal protein S10	ribosomal protein S10	rib

GENE NAME	RefSeq	LUA TAG	PROBE SEQUENCE
G0S2	NM_015714	2	5' -TAATACGACTCACTATAGGGCTTTATCAATACATACTACAATCATAGAAGTACCTACCACAAG-3' 5' -Phos-CATCCACCAAAGGAGTTTGGTCCCTTTAGTGAGGGTTAAT-3'
SLC2A3	NM_006931	5	5' -TAATACGACTCACTATAGGGCAATCAAATCACAATAATCAATCACTTCATGTCAACTTTCTGG-3' 5' -Phos-CTCCTCAAACAGTAGTGGTCCCTTTAGTGAGGGTTAAT-3'
S100P	NM_005980	16	5' -TAATACGACTCACTATAGGGAATCAATCTTCATTCAAATCATCATCACAGATTCTGGCAGAGC-3' 5' -Phos-CATGGTCCCAGGCTTCCCAATCCCTTTAGTGAGGGTTAAT-3'
HSPB1	NM_001540	24	5' -TAATACGACTCACTATAGGGTCAATTACCTTTTCAATACAATACAAATCCGATGAGACTGCCGC-3' 5' -Phos-CAAGTAAAGCCTTAGCCTGGTCCCTTTAGTGAGGGTTAAT-3'
PRTN3	NM_002777	25	5' -TAATACGACTCACTATAGGGCTTTTCAATTACTTCAAATCTTCAGGCGGATCTTTGGACAGAAG-3' 5' -Phos-CAGCTTTCCCGAACACTGTCCCTTTAGTGAGGGTTAAT-3'
CALR	NM_004343	30	5' -TAATACGACTCACTATAGGGTACCTTTTATACCTTTCTTTTACGGGTGGACTGAGGCCTGAG-3' 5' -Phos-CGCTCCTGCCAGAGCTTGTCCTTTAGTGAGGGTTAAT-3'
SERPINA1	NM_000295	31	5' -TAATACGACTCACTATAGGGTTCACTTTTCAATCAACTTTAATCTTACATTTACCCAAACTGTC-3' 5' -Phos-CATTACTGGAACCTATGATCTCCCTTTAGTGAGGGTTAAT-3'
GAPDH	NM_002046	32	5' -TAATACGACTCACTATAGGATTTACTACTCAAATAATCTACCCCTGAAGAGGGGAGGG-3' 5' -Phos-CCTAGGGAGCCGACCTTGTCCCTTTAGTGAGGGTTAAT-3'
ACTB	NM_001101	33	5' -TAATACGACTCACTATAGGGTCAATTACTTCACTTTAATCCTTTCTCCCAAGTCCACACAG-3' 5' -Phos-GGGAGTGATAGCATTGCTTTCCCTTTAGTGAGGGTTAAT-3'
RPLP0	NM_001002	34	5' -TAATACGACTCACTATAGGGTCATTCATATACATAACCAATTCATAACTTAGCCAGTTTTATTTG-3' 5' -Phos-CAAAACAAGGAAATAAAGGCTCCCTTTAGTGAGGGTTAAT-3'
FUCA1	NM_000147	29	5' -TAATACGACTCACTATAGGGAATCTTACTACAATCCCTTCTTTGGAAAAGGCTTACCAGGCTG-3' 5' -Phos-CTATGGTCAACTCTTCAGAATCCCTTTAGTGAGGGTTAAT-3'
ALOX5	NM_000698	14	5' -TAATACGACTCACTATAGGGCTACTATACATCTTACTATACTTTCTCAGCATTTCACACCAAG-3' 5' -Phos-CAGCAACAGCAAATCAGACTCCCTTTAGTGAGGGTTAAT-3'
NPC2	NM_006432	27	5' -TAATACGACTCACTATAGGGCTTTTCAAATCAACTCAACTTCAGAAACTGAGCTCCGGGTG-3' 5' -Phos-GCTGGTTCTCAGTGGTTGTCCCTTTAGTGAGGGTTAAT-3'
FCER1G	NM_004106	44	5' -TAATACGACTCACTATAGGGTCATTTACCAATCTTTCTTTATACCCAGGAACCAGGAGACTTAC-3' 5' -Phos-GAGACTCTGAAGCATGAGAATCCCTTTAGTGAGGGTTAAT-3'
TYROBP	NM_003332	43	5' -TAATACGACTCACTATAGGGCTTTCAATTACAATACTCATTACAGAGTGCCATCCCTGAGAGAC-3' 5' -Phos-CAGACGCTCCCAATACTCTCCCTTTAGTGAGGGTTAAT-3'
NCF2	NM_000433	28	5' -TAATACGACTCACTATAGGGCTACAACAACAAACATTATCAAAGGGCAGAGAGTCTTC-3' 5' -Phos-CAGTACTGATCCTGTTCTTCCCTTTAGTGAGGGTTAAT-3'
ITGAM	NM_000632	12	5' -TAATACGACTCACTATAGGGTACACTTTCTTTCTTTCTTTCTTTGGTTTCCTTCAGACAGATTC-3' 5' -Phos-CAGGCGATGTGCAAGTGTATCCCTTTAGTGAGGGTTAAT-3'
ITGB2	NM_000211	39	5' -TAATACGACTCACTATAGGGTACACAATCTTTTCATTACATCATAGAAATCCAGTTATTTCCG-3' 5' -Phos-CCCTCAAATGACAGCCATGTCCTTTAGTGAGGGTTAAT-3'
MPO	NM_000250	87	5' -TAATACGACTCACTATAGGAACTAACATCAATACTTACATATTCTCCACCTGATTTCTTG-3' 5' -Phos-CTTATTCAGTGAAGTTCTCCCTTTAGTGAGGGTTAAT-3'

**Table S2. Primary RNAi screen signature genes (19-gene signature)**

Listed are the gene names, Ref Seq numbers, Luminex LUA tags, and the probe sequence for the 19 myeloid differentiation signature genes used in the primary RNAi screen.

GENE NAME	RefSeq	LUA TAG	PROBE SEQUENCE
RGS2	NM_002923	1	5'-TAATACGACTCACTATAGGGCTTTAATCTCAATCAATACAAATCAGGGAATAGGTGGTCTGAAC-3' 5'-Phos-GTGGTGTCTCACTCTGAAAAATCCCTTTAGTGAGGGTTAAT-3'
NCF1	NM_000265	2	5'-TAATACGACTCACTATAGGGCTTTATCAATACATACTACAATCATGGACGCCGAGGGCAGCCCC-3' 5'-Phos-GACCCCTGTCCAGCGCGGCTTCCCTTTAGTGAGGGTTAAT-3'
KIAA0513	NM_014732	3	5'-TAATACGACTCACTATAGGGTACACTTTATCAAATCTTACAATCCACCAGTATCTTCTGTGTG-3' 5'-Phos/CATTTTGCATCTTGTGTCTCCCTTTAGTGAGGGTTAAT-3'
IER3	NM_003897	4	5'-TAATACGACTCACTATAGGGTACATTACCAATAATCTTCAAATCGCTGTACGGAGCGACTGTC-3' 5'-Phos-GAGATCGCCTAGTATGTTCTTCCCTTTAGTGAGGGTTAAT-3'
EMR3	NM_032571	5	5'-TAATACGACTCACTATAGGGCAATTCAAATCACAATAATCAATCGATGGGTCTGACTCAAAAC-3' 5'-Phos-CCAGTGAGGGGATGTTTTTCCCTTTAGTGAGGGTTAAT-3'
KIAA0913	NM_015037	9	5'-TAATACGACTCACTATAGGGTAATCTTCTATATCAACATCTTACTGGGAGGGGCGTTGGGTGG-3' 5'-Phos-CCTCTGGTATTTATTGGCATCCCTTTAGTGAGGGTTAAT-3'
CYP4F3	NM_000896	15	5'-TAATACGACTCACTATAGGATACTTCATTTCATCAATTCATCTGGATTTCTATCTATTC-3' 5'-Phos-CATGTTGGACCAATACCACATCCCTTTAGTGAGGGTTAAT-3'
PSMG1	NM_003720	24	5'-TAATACGACTCACTATAGGGCAATTCCTTTTCAAACAATAACAACAACCAATATAGTACAC-3' 5'-Phos-GACCTTCTGACAGCAGTCTTCCCTTTAGTGAGGGTTAAT-3'
NPM1	NM_002520	25	5'-TAATACGACTCACTATAGGGCTTTCAATTACTTCAAATCTTCATGATAGGACATAGTAGTAGC-3' 5'-Phos-GGTGGTCAGACATGGAATGTCCTTTAGTGAGGGTTAAT-3'
PEBP1	NM_002567	26	5'-TAATACGACTCACTATAGGGTACTCAAATCTACACTTTTTCAGAAAAGCTGGTCTGGAGTTG-3' 5'-Phos-CTGAATGTGCATTAATTGTTCCCTTTAGTGAGGGTTAAT-3'
ANP32E	NM_030920	27	5'-TAATACGACTCACTATAGGAAAGTTGAGTATTGATTTGAAAAGATATTTGTAGAAGTTTTCG-3' 5'-Phos-GTCTTATTTAATGCTTTTGTCCCTTTAGTGAGGGTTAAT-3'
BCLAF1	NM_001077440	31	5'-TAATACGACTCACTATAGGGTCACTTTTCAATCAACTTTAATCAAATACTCACTGATACCTG-3' 5'-Phos-CGTAAACATACTTTGTTTTGTCCTTTAGTGAGGGTTAAT-3'
LAS1L	NM_031206	35	5'-TAATACGACTCACTATAGGGCAATTCATCATTTCATTTTCATGGAGACAGCCTGGATCAG-3' 5'-Phos-CCACATCAACTCAGTTGTCCTCCCTTTAGTGAGGGTTAAT-3'
MPO	NM_000250	40	5'-TAATACGACTCACTATAGGGCTTTCTACATTATTACAACATTATTCCTCACCTGATTTCTTG-3' 5'-Phos-CTTATTCACTGAAGTCTCCTCCCTTTAGTGAGGGTTAAT-3'
HSP90B1	NM_003299	42	5'-TAATACGACTCACTATAGGGCTATCTTCATATTTCACTATAAACGGAGAGACTGTTTTGGATG-3' 5'-Phos-CCCCCTAATCCCTTCTCCCTCCCTTTAGTGAGGGTTAAT-3'
GINS2	NM_016095	43	5'-TAATACGACTCACTATAGGGCTTTCAATTAACAATACTCATTACAGCCAACAATGCTGACCGGTG-3' 5'-Phos-CTTATCTCTAAGCCCTGATTCCTTTAGTGAGGGTTAAT-3'
RRP7A	NM_015703	45	5'-TAATACGACTCACTATAGGGTCAATTCACAATCAATTACTCAACCTCAATGCAAAAAGCCCTTG-3' 5'-Phos-CTGGCAACGAAAAAGCCTCATCCCTTTAGTGAGGGTTAAT-3'
PRTN3	NM_002777	51	5'-TAATACGACTCACTATAGGGTCAATTCATCAATCATCAACAATCTTCGTGATCTGGGGATGTG-3' 5'-Phos-CCACCCGCTTTTCCCTGACTCCCTTTAGTGAGGGTTAAT-3'
HSPB1	NM_001537	95	5'-TAATACGACTCACTATAGGGTACACTTTAAACTTACTACACTAAAAATCCGATGAGACTGCCG-3' 5'-Phos-CAAGTAAAGCCTTAGCCCTGGTCCCTTTAGTGAGGGTTAAT-3'
G0S2	NM_015714	92	5'-TAATACGACTCACTATAGGGCTATTACACTTTAAACATCAATACTAGAAGTACCTACCACAAG-3' 5'-Phos-CATCCCAAAAGGAGTTTGGTCCCTTTAGTGAGGGTTAAT-3'
SLC2A3	NM_006931	93	5'-TAATACGACTCACTATAGGGCTTCTATTCATCTAATAACAAACACTTCATGTCAACTTCTTG-3' 5'-Phos-CTCCTCAACAGTAGGTTGGTCCCTTTAGTGAGGGTTAAT-3'
S100P	NM_005980	94	5'-TAATACGACTCACTATAGGGCTTTCTATCTTCTACTCAATAATTCACAGATTCCTGGCAGAGC-3' 5'-Phos-CATGGTCCAGGCTTCCCAATCCCTTTAGTGAGGGTTAAT-3'
SERPINA1	NM_000295	98	5'-TAATACGACTCACTATAGGGAATCATACTCAACTAATCATTCAATTACATTTACCCAAACTGTC-3' 5'-Phos-CATTACTGGAACCTATGATCTCCCTTTAGTGAGGGTTAAT-3'
FUCA1	NM_000147	99	5'-TAATACGACTCACTATAGGGAATCTACACTAACAAATTCATAACGGAAAAGGCTTACCAGGCTG-3' 5'-Phos-CTATGGTCAACTCTTCAGAAATCCCTTTAGTGAGGGTTAAT-3'
ALOX5	NM_000698	14	5'-TAATACGACTCACTATAGGGCTACTATACATCTTACTATACTTCTCAGCATTTCCACACCAAG-3' 5'-Phos-CAGCAACAGCAAAATCAGCACTCCCTTTAGTGAGGGTTAAT-3'
NPC2	NM_006432	96	5'-TAATACGACTCACTATAGGGATACTAACTCAACTAACTTTAAACCAGAAACTGAGCTCCGGGTG-3' 5'-Phos-GCTGGTCTCAGTGGTGTCTCCCTTTAGTGAGGGTTAAT-3'
FCER1G	NM_004106	44	5'-TAATACGACTCACTATAGGGTCAATTTACCAATCTTCTTTATACCCAGGAACCCAGGAGACTTAC-3' 5'-Phos-GAGACTCTGAAGCATGAGAATCCCTTTAGTGAGGGTTAAT-3'
NCF2	NM_000433	28	5'-TAATACGACTCACTATAGGGCTACAAAACAACAACATTTATCAAAGGGCAGGAGAGTCTTC-3' 5'-Phos-CAGGTAAGTCTGATCCTGTTTCTCCCTTTAGTGAGGGTTAAT-3'
ITGAM	NM_000632	12	5'-TAATACGACTCACTATAGGGTACACTTTCTTCTTCTTCTTCTTGGTTTCTTTCAGACAGATTC-3' 5'-Phos-CAGGCGATGTGCAAGTATTCCCTTTAGTGAGGGTTAAT-3'
ITGB2	NM_000211	39	5'-TAATACGACTCACTATAGGGTACACAATCTTTTCATTACATCATAGAAATCCAGTTATTTTCCG-3' 5'-Phos-CCCTCAAATGACAGCCATGTCCTTTAGTGAGGGTTAAT-3'
GAPDH	NM_002046	34	5'-TAATACGACTCACTATAGGGTCAATTCATATACATAACCAATTCATATCTCCCTCTCACAGTTG-3' 5'-Phos-CCATGTAGACCCCTTGAAGATCCCTTTAGTGAGGGTTAAT-3'
HNRNPAB	NM_031266	52	5'-TAATACGACTCACTATAGGGTCAATCATCTTTATACTTCACAATGCCTGGACCTGTGGACCTG-3' 5'-Phos-GTTGTAAGAGTAAATGTATCCCTTTAGTGAGGGTTAAT-3'

**Table S3. Differentiation signature (32-gene signature).** Listed are the gene names, Ref Seq numbers, Luminex LUA tags, and the probe sequence for the 32 myeloid differentiation signature genes.

<b>Cell Line</b>	<b>Day 3 IC50 (µM)</b>
MOLM-14	0.026
Kasumi-1	0.207
KG-1	0.406
THP-1	>10
U937	3.43
HL-60	5.5

**Table S4. AML cell line R406 viability IC<sub>50</sub>**

AML cell lines were treated in a minimum of four replicates and viability measured at three days with an ATP-based assay. Values for IC<sub>50</sub> (drug concentrations that reduced cell viability to 50 percent of the vehicle controls) were calculated using a natural cubic spline fit to the measured viability data in R (using the spline function).

<b>Pre-B- ALL</b>	<b>Day 3 IC50 (μM)</b>
697	6.15
NALM-6	4.50
REH	> 10
RS4-11	> 10
SEMK2	0.28
SUP-B15	> 10

<b>T- ALL</b>	<b>Day 3 IC50 (μM)</b>
DND-41	> 10
HPB-ALL	> 10
KOPTK1	1.28
MOLT-4	6.16
PF-382	7.50

**Table S5. ALL cell line R406 viability IC<sub>50</sub>**

ALL cell lines were treated with R406 and viability measured at three days with an ATP-based assay. Values for IC<sub>50</sub> (drug concentrations that reduced cell viability to 50 percent of the vehicle controls) were calculated using a natural cubic spline fit to the measured viability data in R (using the spline function). Values reported represent the mean of at least two independent experiments in which each experiment included a minimum of six replicates for each condition.



Hairpin Name	Gene Symbol	RefSeq ID	TRC ID #	shRNA Oligonucleotide Sequence
Syk_1	SYK	NM_003177	TRCN0000003163	CCGGGCAGGCCATCATCAGTCAGAACTCGAGTTCTGACTGATGATGGCCTGCTTTTT
Syk_7	SYK	NM_003177	TRCN0000195465	CCGGCAGAGGAATTTGGCTGCTTCTCTCGAGAGAAGCAGCCAAATTCCTCTGTTTTTTG
Syk_10	SYK	NM_003177	TRCN0000197257	CCGGGCAGCAGAACAGACATGTCAACTCGAGTTGACATGTCTGTTCTGCTGCTTTTTTG

### Table S6. Syk shRNA sequence

Hairpin sequence for the three *SYK*-directed hairpins reported in the manuscript.